

RESEARCH ARTICLE

The polycomb component Ring1B regulates the timed termination of subcerebral projection neuron production during mouse neocortical development

Nao Morimoto-Suzuki^{1,2}, Yusuke Hirabayashi^{2,*}, Kelsey Tyssowski², Jun Shinga³, Miguel Vidal^{3,4}, Haruhiko Koseki³ and Yukiko Gotoh^{1,2,*}

ABSTRACT

In the developing neocortex, neural precursor cells (NPCs) sequentially generate various neuronal subtypes in a defined order. Although the precise timing of the NPC fate switches is essential for determining the number of neurons of each subtype and for precisely generating the cortical layer structure, the molecular mechanisms underlying these switches are largely unknown. Here, we show that epigenetic regulation through Ring1B, an essential component of polycomb group (PcG) complex proteins, plays a key role in terminating NPC-mediated production of subcerebral projection neurons (SCPNs). The level of histone H3 residue K27 trimethylation at and Ring1B binding to the promoter of *Fezf2*, a fate determinant of SCPNs, increased in NPCs as *Fezf2* expression decreased. Moreover, deletion of *Ring1B* in NPCs, but not in postmitotic neurons, prolonged the expression of *Fezf2* and the generation of SCPNs that were positive for CTIP2. These results indicate that Ring1B mediates the timed termination of *Fezf2* expression and thereby regulates the number of SCPNs.

KEY WORDS: Neocortical development, *Fezf2*, Polycomb, Neural stem cell, Neural precursor cell

INTRODUCTION

The mammalian neocortex contains various types of projection neurons, which are finely organized into a laminar structure. Projection neurons can be classified using their somal location, dendritic arborization and targets of axonal projection (Kwan et al., 2012; O'Leary and Koester, 1993). Intracortical projection neurons are located in both superficial and deep layers, whereas corticofugal projection neurons, such as subcerebral projection neurons (SCPNs), which form connections with subcerebral targets, are confined to deep cortical layers V and VI (Kwan et al., 2012; Molyneaux et al., 2007). SCPNs vary in number between cortical areas (Arlotta et al., 2005; Polleux et al., 1997), and the regulation of the number of SCPNs might be important in determining the function of some areas. For example, the primary motor area contains a relatively large number of SCPNs (such as those responsible for the pyramidal tract) that are essential for its motor-

associated functions. Furthermore, the development of SCPNs is a focus of clinical interest because these neurons degenerate in response to spinal cord injury, and in some neurodegenerative diseases, such as amyotrophic lateral sclerosis (ALS), they contribute to the malfunction of the motor system (Pasinelli and Brown, 2006).

The developing mouse neocortex contains multipotent neural precursor cells (NPCs) (McConnell and Kaznowski, 1991; Noctor et al., 2001; Guo et al., 2013; Franco et al., 2012), and these NPCs collectively produce various neuronal subtypes and then glial cells in a defined temporal order (Qian et al., 2000; Shen et al., 2006). The length of time for which NPCs produce each cell type is crucial for determining the cell composition (Polleux et al., 1997) – e.g. delayed termination of the production of a certain cell type would increase the number of cells of this type. Because newborn neurons migrate radially toward the pia and settle outside of earlier born neurons, the temporal order of the generation of neuronal subtypes from NPCs roughly corresponds to their spatial order within the cortical plate (Ayala et al., 2007; Kohwi and Doe, 2013; Kriegstein and Noctor, 2004). Deep cortical layers, including SCPNs, are thus generated early in neocortical development [from 12.5 to 14 days post coitum (dpc)] (Hevner et al., 2003; Molyneaux et al., 2007). Extrinsic signals can affect the fate transitions of NPCs, given that early-stage NPCs adopt a late-stage fate when grafted into a late-stage neocortex (McConnell and Kaznowski, 1991). Interestingly, late-stage NPCs do not regain an early-stage fate when grafted into an early-stage neocortex, indicating a loss of the differentiation competence during the course of development [see the ‘progressive fate restriction’ model (Desai and McConnell, 2000)]. Together with previous reports showing that microcultures of neocortical NPCs exhibit the sequential fate switches in a similar order to those observed *in vivo* (Shen et al., 2006), these studies indicate that cell intrinsic mechanisms in NPCs, at least in part, govern the fate switches and maintain the limited competence of NPCs.

Although some of the molecules responsible for the generation of particular neuronal subtypes by NPCs have been identified, such as *Foxg1* and COUP-TF (Hanashima et al., 2004; Naka et al., 2008), little is known about how the timing of the expression of these molecules is regulated to govern the fate switches during development. As for the specification of SCPNs, the transcription factor *Fez* family zinc-finger 2 (*Fezf2*) has been identified as a key player (Chen et al., 2005a,b; Molyneaux et al., 2005). The expression of *Fezf2* is induced in early-stage NPCs when they produce SCPNs, and ablation of *Fezf2* results in the loss of all SCPNs. When *Fezf2* is misexpressed in late-stage NPCs or immature neurons that would normally generate superficial layer neurons, they ectopically produce neurons with molecular markers and axonal projections characteristic of SCPNs (Chen et al., 2005a,b; De la

¹Graduate School of Pharmaceutical Sciences, The University of Tokyo, Tokyo, Japan. ²Institute of Molecular and Cellular Biosciences, The University of Tokyo, Tokyo, Japan. ³RIKEN Center for Allergy and Immunology, Kanagawa, Japan. ⁴Centro de Investigaciones Biológicas, Consejo Superior de Investigaciones Científicas, Madrid, Spain.

*Authors for correspondence (yhira@iam.u-tokyo.ac.jp; ygotoh@mol.f.u-tokyo.ac.jp)

Rossa et al., 2013; Molyneaux et al., 2005; Rouaux and Arlotta, 2013). Thus, the expression level of *Fezf2* determines the neuronal subtype produced. However, it remains elusive as to how the level of *Fezf2* is downregulated when neocortical NPCs stop producing SCPNs during development.

It has become increasingly clear in recent years that epigenetic events govern the cell state and cell fate decisions (Bernstein et al., 2007; Sparmann and van Lohuizen, 2006). Polycomb group (PcG) proteins have emerged as central players in these epigenetic programming events during development (Aldiri and Vetter, 2012; Sauvageau and Sauvageau, 2010; Schwartz and Pirrotta, 2007). PcG proteins are transcription repressors that modulate histones and chromatin structure. They comprise two main complexes, referred to as polycomb repressive complexes 1 and 2 (PRC1 and PRC2). PRC2 contains Eed, Suz12 and the methyltransferase Ezh2 (or Ezh1) that catalyzes trimethylation of residue Lys27 of histone H3 (H3K27me3) (Cao and Zhang, 2004; Margueron and Reinberg, 2011). This histone modification then provides a platform to recruit PRC1, which contains the ubiquitin ligase Ring1 (Ring1A; Ring1 – Mouse Genome Informatics; or Ring1B; Rnf2 – Mouse Genome Informatics) (de Napoles et al., 2004). PcG proteins mediate the neurogenic-to-gliogenic switch of NPC fate in the late stage of neocortical development (Hirabayashi et al., 2009; Sparmann et al., 2013) and the progressive loss of competence to generate early-born neurons in *Drosophila* neuroblasts (Touma et al., 2012). However, their roles in regulating the switches of neuronal subtypes during the mammalian neurogenic phase have remained unclear.

In this study, we show that epigenetic regulation by the PcG protein Ring1B plays an essential role in terminating the production of layer V SCPNs at the correct developmental time. We found that the level of H3K27me3 and Ring1B binding at the *Fezf2* locus in NPCs increases as *Fezf2* expression is reduced. In mouse neocortical NPCs lacking *Ring1B*, *Fezf2* expression was induced even in the late stage, resulting in the prolonged production of SCPNs. Our findings reveal that the timed termination of SCPN fate

by PcG proteins is crucial for determining the number of neurons of this subtype.

RESULTS

Deletion of Ring1B in NPCs increases the number of neurons that are CTIP2⁺⁺ in the neocortex

The role of PcG complexes in the neurogenic-to-gliogenic transition of NPC fate in the perinatal neocortex prompted us to investigate their role in the neuronal subtype regulation of NPC fate during the neurogenic phase in the late embryonic neocortex. We thus conditionally deleted the *Ring1B* gene, a central component of PRC1, in NPCs *in vivo* by crossing *Ring1B^{fllox/fllox}* mice with mice harboring a Nestin-CreERT2 transgene (*NesCreERT2*), which expresses the *CreERT2* gene under the control of the NPC-specific Nestin enhancer (Imayoshi et al., 2006). We confirmed that a single intraperitoneal injection of tamoxifen into a pregnant mouse at 13 dpc induced genomic recombination of the *Ring1B* gene and reduced the amount of Ring1B protein to an undetectable level in neurons in layers II to V, which are generated after 13 dpc (Fig. 1A,B). At birth, *Ring1B^{fllox/fllox};NesCreERT2* mice that had been injected with tamoxifen at 13 dpc exhibited six-layered cortices similar in size to control cortices. We first examined the composition of neuronal subtypes within the primary somatosensory (S1) area through immunohistochemistry using mice at 18.5 dpc or postnatal day 2 (P2). Ring1B deletion by using tamoxifen injection at 13 dpc did not markedly change the number of layer VI neurons that were positive for *Tbr1*, or that of neurons that were weakly positive for CTIP2 (*BCL11B* – Mouse Genome Informatics), which are normally generated before 13 dpc (Fig. 1C,D; supplementary material Fig. S1A,B). By contrast, Ring1B deletion under the same condition significantly increased the number of layer V SCPNs that expressed CTIP2 at high levels (CTIP2⁺⁺) (Fig. 1C,D,G). The number of CTIP2⁺⁺ cells in the S1 area reproducibly exhibited more than a 30% increase in Ring1B-deficient mice compared with that of control mice. Moreover, Ring1B deletion reduced the number

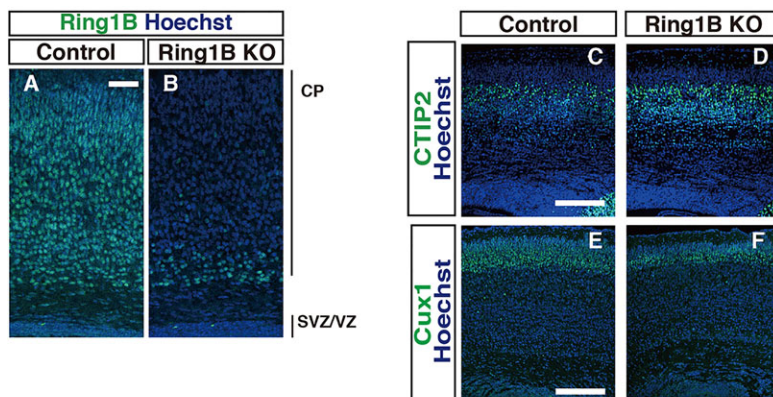
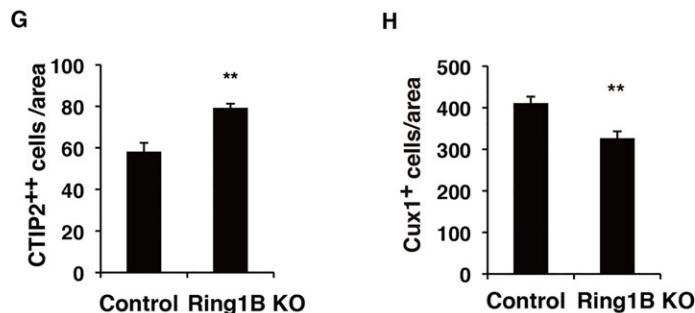


Fig. 1. Deletion of Ring1B in NPCs increases the number of CTIP2⁺⁺ cells in the neocortex and decreases the number of Cux1-positive cells. Control (A,C,E) or *Ring1B^{fllox/fllox}*, *NesCreERT2* (B,D,F) mice were treated with tamoxifen at 13.0 dpc. The pups' brains were fixed at P2 (A,B,E,F) or 18.5 dpc (C,D) and subjected to immunohistochemistry with the antibodies indicated. The number of CTIP2⁺⁺ cells or Cux1⁺ cells (G,H) were determined. The S1 area is shown. Data are the means±s.e.m. of values of six corresponding areas of three control mice and eight corresponding areas of four knockout (KO) mice (G) and of eight corresponding areas of four hemispheres (H). See also supplementary material Fig. S1. ***P*<0.01. CP, cortical plate; Hoechst, Hoechst 33342; SVZ, subventricular zone; VZ, ventricular zone. Scale bars: 50 μm (A), 100 μm (C,E).



of superficial layer neurons that expressed Cux1 by 21% in P2 neocortex (Fig. 1E,F,H), and none of the increased number of CTIP2⁺⁺ neurons in Ring1B knockout mice expressed Cux1 (supplementary material Fig. S1E–J). We further investigated whether Ring1B knockout affects the number of layer V callosal projection neurons (CPNs) that are produced during the same period as layer V SCPNs. We thus examined the number of cells that were positive for Satb2, a CPN marker (Alcamo et al., 2008; Britanova et al., 2008; Leone et al., 2008), and located in layer V. We found that deletion of Ring1B did not significantly change the number of Satb2-positive cells located in layer V at stage E18 or P2, when Stab2-positive cells settle in layer V (supplementary material Figs S1C,D and S2A,D), suggesting that Ring1B does not largely affect the production of CPNs in layer V. These results indicate that Ring1B plays a role in controlling the composition of neuronal subtypes in the developing neocortex by reducing the number of CTIP2⁺⁺ neurons.

A Ring1B-dependent developmental fate switch takes place in NPCs but not in postmitotic neurons

Previous studies have indicated that the subtype specification of neurons during neocortical development can take place in both NPCs and postmitotic neurons (Bedogni et al., 2010; Fishell and Hanashima, 2008; Han et al., 2011; Joshi et al., 2008; Leone et al., 2008). Some of the molecules involved in neuronal subtype specification are expressed primarily in the postmitotic neurons, supporting that neuronal subtype determination occurs at a postmitotic stage. Moreover, a recent study has shown that postmitotic misexpression of Fezf2, a fate determinant of layer V SCPNs, resulted in the reprogramming of upper layer neurons into SCPNs, suggesting that neuronal phenotypes can be reprogrammed even in postmitotic immature neurons (De la Rossa et al., 2013; Rouaux and Arlotta, 2013). However, it remains unclear whether the SCPN fate is normally determined within NPCs or neurons during neocortical development. We therefore asked whether the increased number of CTIP2⁺⁺ neurons in Ring1B-deficient mice was due to the function of Ring1B in NPCs or that in neurons. To examine this, we deleted Ring1B in the neocortex by crossing Ring1B^{lox/lox} mice with NEX-Cre mice, which express Cre recombinase in differentiating neurons under the control of the *Math2* (*Neurod6* – Mouse Genome Informatics) promoter (Goebbels et al., 2006; Wu et al., 2005). In this mouse line (Ring1B^{lox/lox};NEX-Cre), the amount of Ring1B protein compared with that in controls was substantially lower in postmitotic neurons but not in the ventricular zone (VZ), where NPCs reside (supplementary material Fig. S3A,B). However, we found that the numbers of CTIP2⁺⁺ neurons and Cux1-positive neurons per unit width (per column) in Ring1B^{lox/lox};NEX-Cre mice at P0 and P2 were similar to those in control mice (supplementary material Fig. S3C–K). Therefore, conditional deletion of Ring1B specifically in postmitotic neurons is not sufficient to increase the number of CTIP2⁺⁺ neurons and decrease that of Cux1-positive neurons. This suggests that the increased number of CTIP2⁺⁺ neurons in Ring1B-deficient mice resulted from the action of Ring1B in undifferentiated NPCs rather than in postmitotic neurons.

Deletion of Ring1B does not promote premature cell cycle exit and differentiation of NPCs

The increase in the number of CTIP2⁺⁺ neurons in Ring1B-deficient mice could be explained by several possibilities, including the extended period of CTIP2⁺⁺ production and the premature differentiation of NPCs during the period of CTIP2⁺⁺ neuron

production. Premature differentiation could also result in the exhaustion of NPCs and the reduction of late-born neurons, including Cux1-positive neurons. Indeed, a previous report has shown that an earlier (around 9.5 dpc) deletion of Ezh2 in NPCs or knockdown of another PRC1 component, Bmi1 (at around 11 dpc), suppresses the maintenance of NPCs (Fasano et al., 2007, 2009; Pereira et al., 2010). However, we found that Ring1B deletion at the later stages examined in this study (Ring1B^{lox/lox};NesCreERT2 mice injected with tamoxifen at 13.0–13.5 dpc) did not reduce the number of Pax6-positive undifferentiated NPCs in the VZ at 15.5 dpc or P2 (Fig. 2A–D,K; supplementary material Fig. S4A–C), nor did it increase the number of cells that were positive for β III tubulin (Tubb3 – Mouse Genome Informatics) (Fig. 2I,J), suggesting that Ring1B is not necessary for the maintenance of undifferentiated NPCs at this stage. We also asked whether Ring1B deletion affects the rate of cell cycle exit of NPCs. In this assay, 5-ethynyl-2'-deoxyuridine (EdU) was injected at 14.5 dpc, and the rate of cell cycle exit during a 24 h period, judged by the fraction of cells that were negative for Ki67 (Mki67 – Mouse Genome Informatics) among EdU-positive cells, was examined at 15.5 dpc. We found that Ring1B deletion did not significantly affect the rate of cell cycle exit of proliferating cells within the VZ (Fig. 2N–P). Moreover, we found that Ring1B deletion did not affect the number of the cells that were positive for the M-phase marker phospho-histone H3 (pH3) or the intermediate progenitor marker Tbr2 (Fig. 2E–H,L,M). These results together suggest that Ring1B deletion at this late developmental stage does not substantially suppress the self-renewal of NPCs nor promote the neuronal differentiation that accompanies the cell cycle exit. Therefore, the increase in the number of CTIP2⁺⁺ neurons in the Ring1B-deleted brain observed in this study does not appear to be due to the premature differentiation of NPCs.

Ring1B is necessary for the correct timing of the termination of CTIP2⁺⁺ neuron production

Because we assumed that Ring1B regulates the timing of the restriction of the SCPN fate of NPCs, we performed a 5-bromo-2'-deoxyuridine (BrdU) birthdate analysis to determine whether Ring1B deletion extends the period of CTIP2⁺⁺ neuron production. The production of CTIP2⁺⁺ neurons in the S1 area normally ceases by 14 dpc (Hevner et al., 2003; Molyneux et al., 2007), so when BrdU was injected at 14 dpc, few BrdU-labeled cells were found among the CTIP2⁺⁺ neurons in the S1 area (Fig. 3B). However, when tamoxifen was injected intraperitoneally into pregnant Ring1B^{lox/lox};NesCreERT2 mice at 13.0 dpc to delete the *Ring1B* gene and BrdU was injected at 14.0 dpc, the percentage of neurons that were double-positive for BrdU and CTIP2⁺⁺ at 18.5 dpc was significantly greater in these mice than that in the control siblings (Fig. 3B–F). This result suggests that CTIP2⁺⁺ cells were produced even at 14 dpc in Ring1B-deficient mice, indicating that Ring1B deletion extended the period of CTIP2⁺⁺ neuron production. These results thus indicate that Ring1B plays a role in terminating CTIP2⁺⁺ neuron production at the correct developmental time.

Excessively produced CTIP2⁺⁺ neurons project normally into the pons in Ring1B-deficient mice

Although CTIP2 is a marker for SCPNs (Arlotta et al., 2005), the extended expression of CTIP2 through Ring1B deletion might not necessarily cause an extended production phase of SCPNs. We therefore examined whether excessively produced CTIP2⁺⁺ neurons in Ring1B-deleted mice indeed project into the subcerebral areas

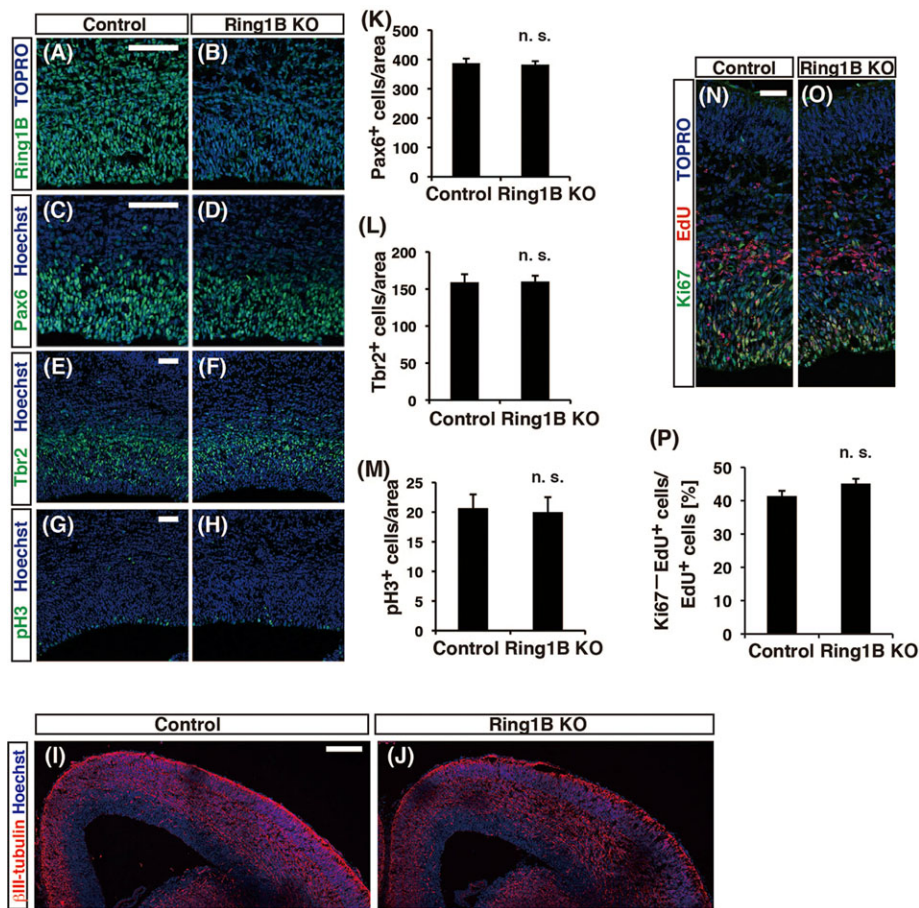


Fig. 2. Knockout of the *Ring1B* gene in NPCs does not affect the number of neural precursor cells. Control mice (A, C, E, G, I, N) or *Ring1B*^{fllox/fllox}; NesCreERT2 (B, D, F, H, J, O) mice were treated with tamoxifen at 13.5 dpc and EdU at 14.5 dpc. The pups' brains were fixed at 15.5 dpc and subjected to immunohistochemistry with the antibodies indicated. (K–M) The number of Pax6-positive (Pax6⁺) cells, Tbr2-positive (Tbr2⁺) cells or pH3-positive (pH3⁺) cells was determined. Data are the means±s.e.m. of values of eight corresponding areas of four control mice and ten corresponding areas of five knockout (KO) mice (K), of six corresponding areas of three control mice and six corresponding areas of three KO mice (L) and of three corresponding areas of three control mice and three corresponding areas of three KO mice (M). (P) The ratio of cells exiting the cell cycle was determined. See also supplementary material Fig. S4. Data are the means±s.e.m. of values of 14 corresponding areas of four control mice and 20 corresponding areas of five KO mice. n.s., not significant. Scale bars: 50 μm.

(i.e. the definition of SCPNs). To this end, we performed retrograde labeling of neurons that extend their axonal terminals into the pons by injecting Alexa Fluor 555-conjugated cholera toxin B subunit (CTB555) into the pons. When CTB555 was injected into the pons at P1, a part of layer V CTIP2⁺⁺ neurons were labeled in a retrograde manner in the S1 area of control mice at P2 as previously described, both in control and in *Ring1B*-deficient mice (Maruoka et al., 2011) (Fig. 3H–O). Importantly, substantial parts of the neurons produced in the ‘extended period’ of CTIP2⁺⁺ neuron production in *Ring1B*-deleted mice, marked by EdU that had been injected at 14.0 dpc, were also labeled in a retrograde manner with CTB555 (Fig. 3I). The percentage of CTB555-labeled cells among EdU-positive CTIP2⁺⁺ neurons in the *Ring1B*-deficient mice was similar to that among EdU-negative CTIP2⁺⁺ neurons (Fig. 3P), suggesting that the CTIP2⁺⁺ neurons produced during the ‘extended period’ in the mutant mice project into the pons normally. This result strongly supports the notion that *Ring1B* plays an essential role in terminating the production of CTIP2⁺⁺ SCPNs in layer V.

Ring1B restricts the expression of *Fezf2* at the time of terminating the production of CTIP2⁺⁺ neurons

Our results suggest that *Ring1B* mediates the termination of CTIP2⁺⁺ neuron production in NPCs rather than in postmitotic neurons. If this is the case, *Ring1B* should regulate its target gene(s) within NPCs in a developmental stage-dependent manner. Because *Fezf2* is a fate determinant of layer V SCPNs and starts to be expressed within the VZ and subventricular zone (SVZ) (Guo et al., 2013; Hirata et al., 2004), we tested whether *Ring1B* and/or other PcG proteins mediate the suppression of *Fezf2* at the time of terminating SCPN production *in vivo*. We directly isolated

undifferentiated NPCs (CD133^{high}, Pax6^{high}, CD133 is also known as Prom1 – Mouse Genome Informatics) and differentiating NPCs (CD133^{mid}, Pax6^{mid}) from the neocortex by using fluorescence-activated cell sorting (FACS) and CD133 immunoreactivity and found that *Fezf2* expression in the CD133^{mid} population was higher than that in CD133^{high} cells at 14 dpc and reduced at 16 dpc (Fig. 4A), consistent with the time of its reported reduction (Hirata et al., 2004). We then deleted *Ring1B* in these NPCs by introducing tamoxifen at 13 dpc into *Ring1B*^{fllox/fllox};NesCreERT2 mice (Fig. 4B,C) and found that this deletion significantly increased the level of *Fezf2* mRNA in CD133^{mid} NPCs (Fig. 4D). We then asked whether the *Fezf2* locus is a direct target of *Ring1B* proteins in NPCs. Because the recruitment of the *Ring1B*-containing complex (PRC1) to its target genomic loci is largely dependent upon the preceding deposition of the histone modification H3K27me3, we examined whether the levels of H3K27me3 and *Ring1B* increase at the *Fezf2* locus at the end of SCPN production, i.e. between 14 and 16 dpc. We found that the levels of both H3K27me3 and *Ring1B* at the *Fezf2* locus in CD133^{high} NPCs were greater at 16 dpc than at 14 dpc, whereas those at other control regions, such as the *Gapdh* locus did not significantly change (Fig. 4E,F). The increased levels of H3K27me3 and *Ring1B* at the *Fezf2* locus without apparent expression of its mRNA in CD133^{high} NPCs suggest that *Ring1B* proteins have already restricted the transcriptional competence (permissiveness) of the *Fezf2* locus in undifferentiated CD133^{high} NPCs at 16 dpc so that the induction of *Fezf2* expression is suppressed in differentiating cells (supplementary material Fig. S8). The level of *Ring1B* mRNA did not increase in CD133^{high} NPCs between 14 and 16 dpc (supplementary material Fig. S6), suggesting that the accumulation of *Ring1B* at the *Fezf2* promoter was not due to

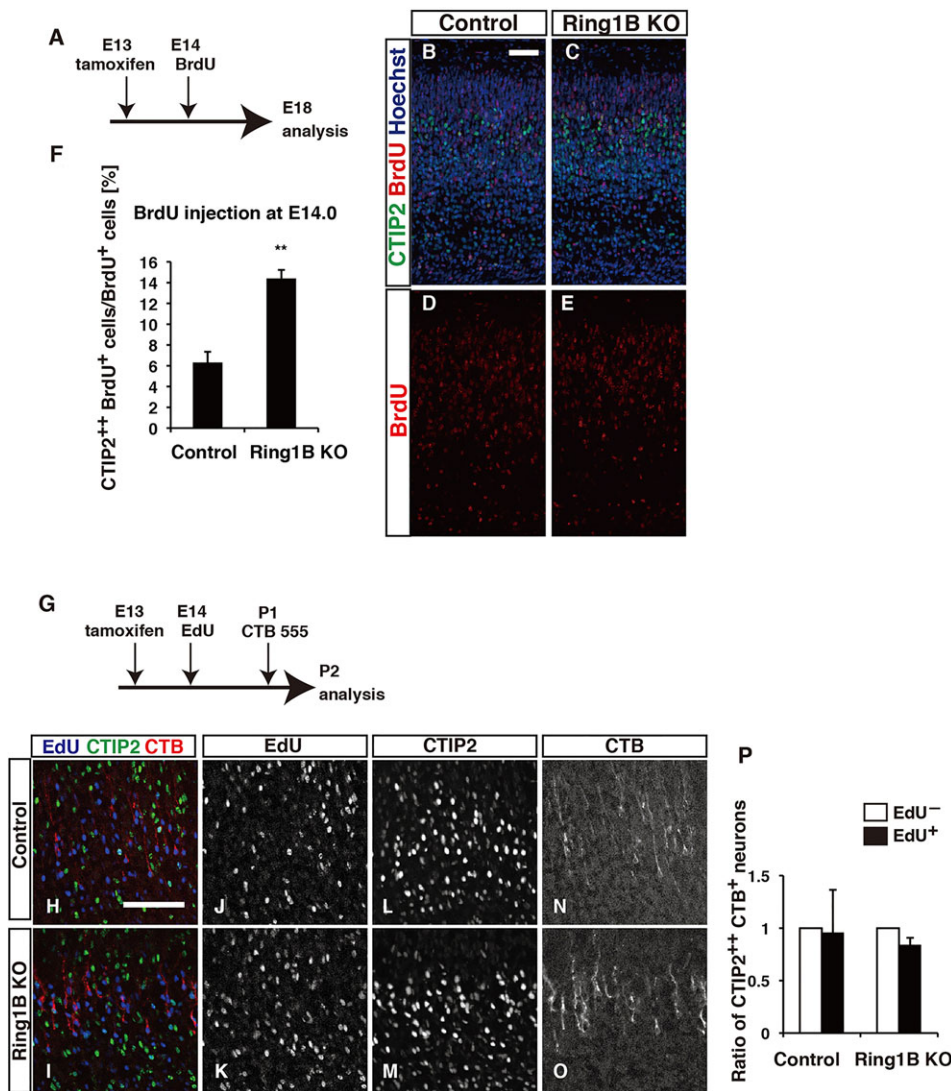


Fig. 3. Ring1B is necessary for the timed termination of layer V CTIP2⁺⁺ neuron production. (A) Experimental schematic of the injection. (B–F) Control (B,D) or Ring1B^{flx/flx};NesCreERT2 (C,E) mice were treated with tamoxifen at 13.0 dpc and BrdU at 14.0 dpc. The pups' brains were fixed at 18.5 dpc and subjected to immunohistochemistry with the antibodies indicated. The number of CTIP2⁺⁺ cells (as described in Fig. 1G) and the percentage of CTIP2⁺⁺ cells among BrdU-positive (BrdU⁺) cells (F) were determined. The S1 areas are shown. Data are the means±s.e.m. of values of six corresponding areas of three control mice and eight corresponding areas of four knockout (KO) mice. (G–P) Excessively produced CTIP2⁺⁺ neurons in Ring1B-deficient mice project normally into the pons. Experimental schematic of the injection. (H–O) Control (H,J,L,N) or Ring1B^{flx/flx};NesCreERT2 (I,K,M,O) mice were treated with tamoxifen at 13.0 dpc and EdU at 14.0 dpc and then treated with CTB555, injected into the pons at P1, fixed at P2 and were then subjected to immunohistochemistry with the antibodies indicated. (P) CTIP2⁺⁺ neurons produced during the 'extended period' in Ring1B KO mice project into the pons. The ratio of CTB555-positive (CTB⁺) and CTIP2⁺⁺ neurons among EdU-negative (EdU⁻) or EdU-positive (EdU⁺) neurons was determined for the pups of Ring1B^{flx/flx};NesCreERT2 mice. Data are means±s.e.m. of values of three control hemispheres and three KO hemispheres. Student's *t*-test, EdU⁺ in Ring1B KO versus those in control. ***P*<0.01. Scale bars: 50 μm.

the increase of Ring1B transcription but was due to the preceding deposition of H3K27me3.

Because dissociation of neocortical NPCs and their isolation by using FACS might affect the chromatin state and gene expression patterns, we also analyzed the cells in the neocortical VZ and SVZ region immediately after manual dissection without the dissociation process. We also confirmed that the expression of *Fezf2* in the VZ and SVZ was reduced (data not shown) and that the level of H3K27me3 was increased at the *Fezf2* locus between 14 and 16 dpc (supplementary material Fig. S7). These results are consistent with those obtained using FACS-isolated NPCs.

Developmental stage-dependent and Ring1B-mediated repression of the *Fezf2* locus in neocortical NPCs

Because previous reports have suggested that the developmental fate switch of NPCs largely depends on cell-intrinsic programs, we wished to examine whether Ring1B also mediates developmental stage-dependent fate switch in isolated NPCs *in vitro* (Eiraku et al., 2008; Gaspard et al., 2008; Shen et al., 2006). NPCs were isolated by culturing neocortical cells from mouse embryos at 11 dpc [0 days *in vitro* (DIV)] in suspension with fibroblast growth factor 2 (FGF2) and epidermal growth factor (EGF) for 3 or 6 DIV (referred to as 3- and 6-DIV cultures, respectively). The fraction of CTIP2-positive

neurons that was induced by an additional 5 days of FGF2 deprivation was reduced between 3 DIV and 6 DIV cultures (Fig. 5A), suggesting that the production of deep layer neurons and SCPNs is terminated between these time points. We found that the levels of H3K27me3 and Ring1B at the *Fezf2* locus were increased in the 6-DIV culture compared with the 3-DIV culture (Fig. 5B,C) and that the expression of *Fezf2* mRNA after 2 h of induction (FGF2 deprivation) was reduced between 3 and 6 DIV (Fig. 5D). Importantly, when Ring1B was conditionally deleted in NPCs isolated from Ring1B^{flx/flx};ERT2-Cre mice by treating them with 4-hydroxy-tamoxifen (4-OHT) for 3 days (Fig. 6A), the level of *Fezf2* mRNA in 6-DIV cultures that had been treated with 4-OHT was significantly higher than that of control cultures that had not been treated with 4-OHT (Fig. 6B), although the treatment with 4-OHT did not change the levels of *Pax6* and *βIII-tubulin* mRNA or the proliferation rate (Fig. 6C–E). Consistent with the derepression of *Fezf2* mRNA, the fraction of CTIP2-positive neurons that was induced upon neuronal differentiation was also greater when Ring1B was conditionally deleted in the 6-DIV culture (Fig. 6F,G). These results support the idea that the *Fezf2* locus is directly repressed by Ring1B proteins within NPCs in a developmental time-dependent manner, even when cultured in isolation.

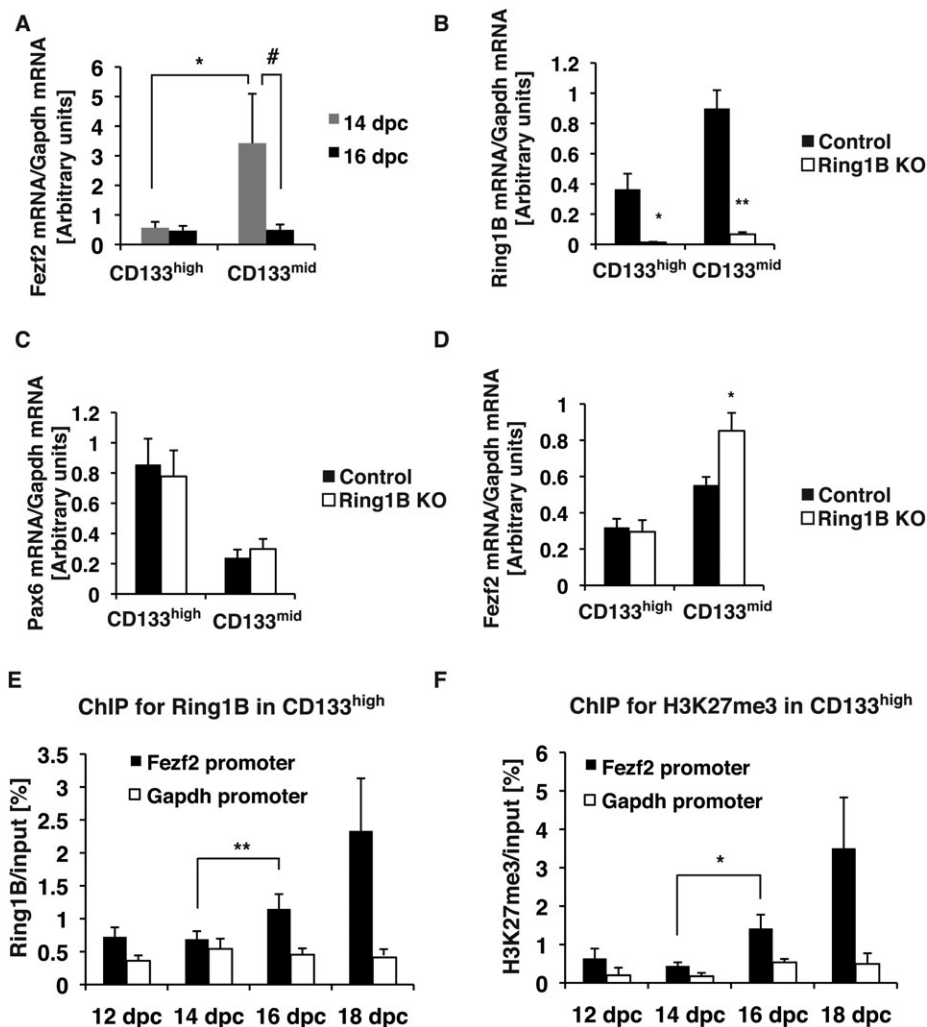


Fig. 4. Ring1B restricted *Fezf2* mRNA expression at the late stage of the neurogenic phase, and H3K27me3 and Ring1B accumulate at the *Fezf2* promoter concurrently with the termination of *Fezf2* mRNA expression. (A) Cells isolated from mouse neocortices at 14 dpc and 16 dpc were stained with an antibody against CD133 and CD133^{high} and CD133^{mid} cells were obtained using FACS (see also supplementary material Fig. S5A,B). The amount of *Fezf2* mRNA was measured by using RT-qPCR. Data are means+s.d. of values from four experiments. (B–D) CD133^{high} and CD133^{mid} cells were obtained from cells isolated from control embryos at 17 dpc and Ring1B^{flx/flx};NesCreER (Ring1B KO) embryos treated with tamoxifen at 13.0 dpc in the same manner as shown in Fig. 5A (supplementary material Fig. S5C–E). The amount of *Ring1B* (B), *Pax6* (C) and *Fezf2* (D) mRNA was measured by using RT-qPCR. Data are means+s.e.m. of values from four control embryos and four KO embryos. (E,F) The chromatin complex was immunoprecipitated, using antibodies against Ring1B and H3K27me3, from CD133^{high} NPCs obtained from each developmental stage using FACS (supplementary material Fig. S5A,B). The amount of H3K27me3 and Ring1B at the *Fezf2* promoter and *Gapdh* promoter was assessed by using qPCR. See also supplementary material Fig. S7. Data are means+s.e.m. of eight experiments (E) and three experiments (F). In F, a one-tailed Student's *t*-test was used. **P*<0.05 for comparison between CD133^{mid} and CD133^{high}, #*P*<0.05 for comparison between 14 dpc and 16 dpc, ***P*<0.01.

***Fezf2* expression mediates the increase in CTIP2-positive neurons upon Ring1B deletion**

Finally, we asked whether the increased expression of *Fezf2* accounts for the increased production of CTIP2-positive neurons upon Ring1B deletion. We thus performed knockdown of *Fezf2* with two independent siRNA oligonucleotide pairs (siFezf2 #1, siFezf2 #2) in cells isolated at 14 dpc and then cultured for 3 DIV. The increase in the percentage of CTIP2-positive neurons upon Ring1B deletion in cells that had been transfected with the control siRNA (siControl) was partially suppressed upon *Fezf2* knockdown (Fig. 6H,I). This result suggests that the suppression of *Fezf2* is responsible for the termination of CTIP2-positive neuron production through Ring1B, at least in part, although we can not rule out that other factor(s) regulated by Ring1B are also involved in the fate specification of SCPNs.

PRC2 component *Ezh2* also represses *Fezf2* expression and CTIP2-positive neuron production

Recent reports (Gao et al., 2012; Leeb et al., 2010; Luis et al., 2012; Schoeftner et al., 2006; Tavares et al., 2012) have shown that Ring1B plays PRC1-independent roles. Therefore, we examined whether the deletion of the *Ezh2* gene, which is a component of PRC2 and is required for the trimethylation of H3K27 in neocortical NPCs (Hirabayashi et al., 2009), affects the expression of *Fezf2* and production of CTIP2-positive neurons *in vitro*, although we could not analyze the effect of *Ezh2* deletion on the timed fate switch of

NPCs *in vivo* owing to the premature differentiation of NPCs (Pereira et al., 2010). We isolated neocortical NPCs from *Ezh2*ΔSET^{flx/flx};ERT2-Cre mice at 12.5 dpc. Treating these NPCs with 4-OHT effectively reduced the amount of intact *Ezh2* mRNA (Fig. 7A). The level of *Fezf2* mRNA and the ratio of CTIP2-positive neurons among total neurons in 6-DIV cultures, isolated at 12.5 dpc, that had been treated with 4-OHT were higher than those of controls (Fig. 7B,D,E). Because the incorporation of BrdU and the ratio of neuronal differentiation in 6-DIV cultures did not significantly change (Fig. 7C,F), these results suggest that deletion of the SET domain of *Ezh2* derepresses *Fezf2* expression but does not result in premature neuronal differentiation under this condition. These results suggest that *Ezh2* is required for the suppression of *Fezf2* in late-stage NPCs.

DISCUSSION

Neocortical NPCs sequentially generate various neuronal subtypes in a defined order within a limited period during development (Molyneaux et al., 2007). Several molecules involved in the subtype specification have been identified, but the mechanisms underlying the NPC transitions from producing one subtype to another have remained largely unclear. Here, we report that the PcG component Ring1B plays an essential role in terminating SCPN production at the correct time during neocortical development. Our results suggest that the termination of SCPN production is mediated by Ring1B-dependent suppression of *Fezf2*, a molecular determinant of SCPN

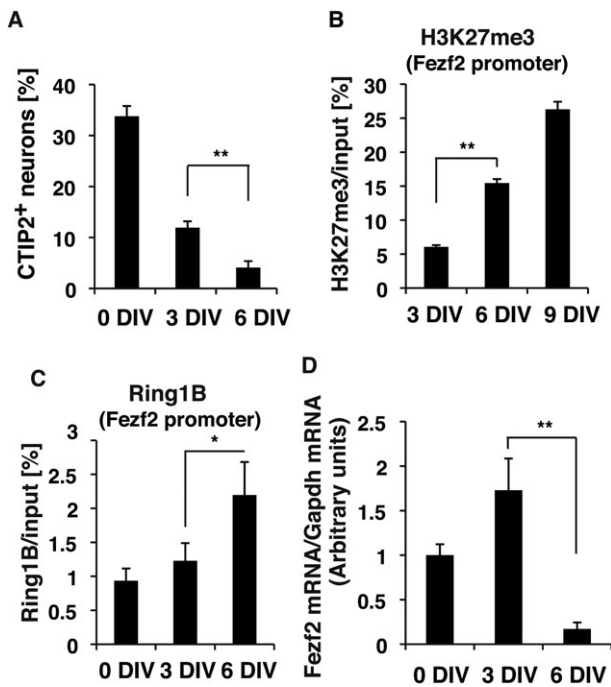


Fig. 5. H3K27me3 and Ring1B accumulate at the *Fezf2* promoter concurrently with the termination of *Fezf2* mRNA expression and CTIP2-positive neuron production *in vitro*. NPCs isolated from embryos at 11 dpc were collected immediately (0) or cultured for 3, 6 or 9 days *in vitro* (DIV). (A) Following each culture period (0, 3 or 6 DIV), cells were plated and cultured for 5 days without FGF2 and EGF. The percentage of CTIP2-positive cells was determined. Data are means±s.e.m. of values from six samples. Similar results were obtained from at least three experiments. (B,C) The chromatin complex was immunoprecipitated with an antibody against H3K27me3 or Ring1B from neocortical NPCs at 11 dpc that had been cultured for the number of days indicated. The amount of H3K27me3 or Ring1B at the *Fezf2* promoter was assessed by using qPCR. Data are means±s.e.m. of three samples (B). Data are means±s.d. of values from three experiments (C). (D) The amount of *Fezf2* mRNA was measured by using RT-qPCR. Data are means±s.d. of values from three experiments. * $P < 0.05$, ** $P < 0.01$.

identity (Chen et al., 2005a,b; Molyneux et al., 2005). The levels of both H3K27me3 and Ring1B protein at the *Fezf2* locus increased as *Fezf2* expression decreased, and Ring1B deletion derepressed *Fezf2* expression. As a result, Ring1B deletion extended the period of production of neurons that were not only CTIP2⁺, a marker for SCPNs, but which also had axons that projected into the pons. We assume that the deletion of Ring1B plays a permissive role, because the termination of SCPNs and the initiation of Cux1-positive neuron production were delayed but still occurred in the Ring1B knockout mice, where a reduction of positive regulator(s) of SCPN production might cause this fate switch. We found that the inactivation of *Ezh2*, an essential component of PRC2, also derepressed *Fezf2* expression and resulted in the increased production of CTIP2-positive neurons in the late-stage neocortical culture. Although we still cannot rule out the possibility that Ring1B acts independently of PcG proteins, this result as well as the timed increase of H3K27me3 at the *Fezf2* locus support the notion that the function of Ring1B in the termination of SCPN production depends on its role as a PcG component.

The function of PcG proteins in suppressing the *Fezf2* locus and terminating SCPN production is reminiscent of their previously described role in suppressing the *Neurog1* locus and thereby terminating neuronal production (Hirabayashi et al., 2009), which takes place later in neocortical development. Therefore, PcG proteins seem to promote the transitions of NPC fate at, at least, two

developmental steps. The roles of PcG proteins in promoting different NPC fate transitions depend on the developmental stages because ablation of the *Ring1B* gene at different stages yielded different phenotypes. Remarkably, Ring1B deletion at an early (mid-gestation) stage slightly reduced the number of Cux1-positive superficial layer neurons (Fig. 1E,F,H), whereas Ring1B deletion at a later (late-gestation) stage increased the number of Cux1-positive neurons, probably because of a delay of the fate switch to gliogenesis (Hirabayashi et al., 2009). This example emphasizes the importance of the timed action of Ring1B in regulating NPC fate.

Then, what mechanism underlies the timed action of Ring1B? Given that the level of H3K27me3 was increased at the *Fezf2* promoter at the termination timing of SCPN production and *Ezh2* were necessary for the changes of NPC fate in our results, it is plausible that PRC1 is recruited to H3K27me3, which is added to different gene loci in NPCs at different times during development. Indeed, the timing of the increase in H3K27me3 differs among Ring1B-target loci, including *Fezf2* and *Neurog1* (supplementary material Fig. S7). Therefore, developmental stage-dependent recruitment of PRC2 to specific loci appears to be important. Although no specific sequence for polycomb recruitment has been identified in mammalian cells, with a few exceptions (Cabanca et al., 2012; Sing et al., 2009; Woo et al., 2010), some transcription factors and non-coding RNAs have been implicated in locus-specific PcG complex recruitment (Guttman and Rinn, 2012; Zhao et al., 2010). Interestingly, an RNA transcribed from an enhancer element of the *Neurog1* locus was found to be necessary for correctly timed *Neurog1* expression (Onoguchi et al., 2012), suggesting a role for RNA in the regulation of PcG proteins in NPCs. It would be interesting to investigate the machinery responsible for the time-, locus- and complex-specific recruitment of PcG proteins in NPCs in future studies.

The different functions of PcG proteins at different developmental stages illustrated above might lend support to the previously proposed ‘progressive fate restriction’ model. Interestingly, a recent report (Touma et al., 2012) has also shown a similar role of PcG proteins in *Drosophila* development. Therefore, PcG proteins might commonly regulate the developmental fate restriction of competence in neural (tissue) stem cells in various organisms and developmental contexts.

Besides SCPNs, layer V contains CPNs (Leone et al., 2008; Molyneux et al., 2007). We found that the numbers of cells expressing *Satb2*, a fate determinant of CPNs (Alcamo et al., 2008; Britanova et al., 2008), and their distribution within the cortical plate were roughly the same between control and Ring1B-deleted neocortices (supplementary material Fig. S2A). Also, Ring1B deletion did not increase the expression of lipoprotein lipase (*Lpl*), another CPN marker in layer V (data not shown). These results indicate that PcG proteins do not terminate layer V CPN production, which seems to make sense because CPNs continue to be produced in layers IV and II and/or III. More markers to distinguish layer-specific CPN are necessary to understand how PcG complexes affect the number of CPN subtypes at each layer.

Although a previous report has shown that the ablation of the *Ezh2* gene compromised the maintenance of undifferentiated NPCs and induced premature differentiation of CTIP2-positive neurons (Pereira et al., 2010; Testa, 2011), Ring1B deletion in the developing neocortex did not cause overt premature differentiation and preserved the undifferentiated Pax6-positive population (supplementary material Fig. S4D-I). This difference might be due to a redundant function of Ring1A (Endoh et al., 2008). We therefore assume that Ring1B is dispensable for the function of *Ezh2* in maintaining NPCs

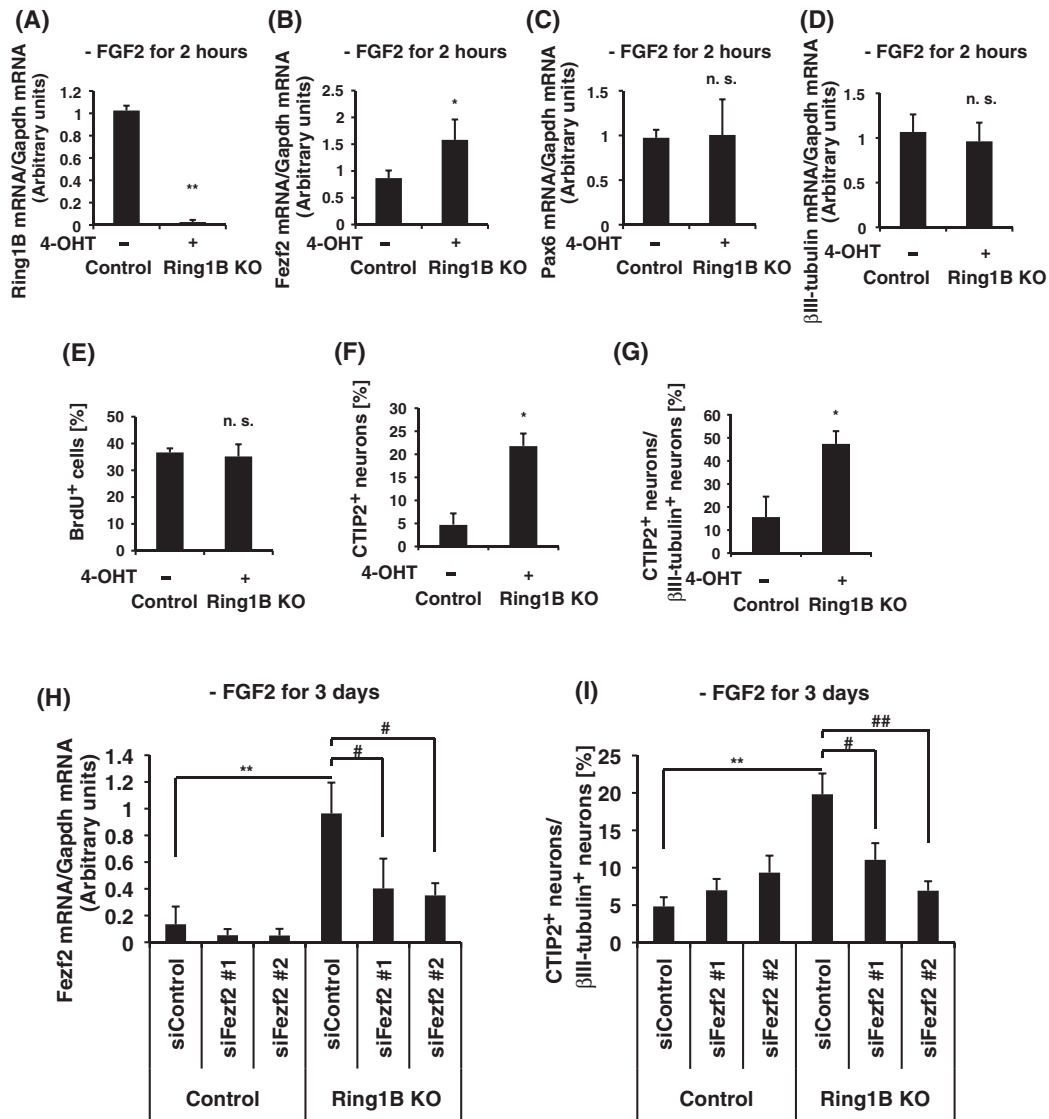


Fig. 6. Knockout of the *Ring1B* gene increases the amount of *Fezf2* mRNA and the percentage of CTIP2-positive neurons *in vitro*. (A–D) *Ring1B* is necessary for the repression of *Fezf2* expression *in vitro*. NPCs isolated from *Ring1B*^{fl^{ox}/fl^{ox}};ERT2-Cre mice at 12.5 dpc were cultured in suspension for 3 days. Then cells were cultured for 3 days with or without 4-hydroxytamoxifen (4-OHT). The amount of the mRNA indicated was measured by using RT-qPCR. Data are means±s.d. of values from five experiments. (E) Knockout (KO) of the *Ring1B* gene did not affect cell proliferation *in vitro*. NPCs isolated from *Ring1B*^{fl^{ox}/fl^{ox}};ERT2-Cre mice at 12.5 dpc were treated as in A. Cells were then treated with BrdU for 30 min, and the percentage of BrdU-positive (BrdU⁺) cells was determined. Data are the means±s.e.m. of values from three samples. (F,G) *Ring1B* regulates the production of CTIP2⁺ neurons *in vitro*. NPCs isolated from *Ring1B*^{fl^{ox}/fl^{ox}};ERT2-Cre mice at 12.5 dpc were treated as in A and cultured for 5 days without FGF2 or EGF. The percentage of CTIP2-positive (CTIP2⁺) cells (F) and CTIP2-positive cells among βIII-tubulin-positive (βIII-tubulin⁺) cells (G) were determined. Data are means±s.e.m. of values from six samples. **P*<0.05, ***P*<0.01. (H,I) *Fezf2* derepression in *Ring1B* KO cells is responsible for the increase in the percentage of CTIP2-positive cells *in vitro*. NPCs isolated from 14.5 dpc *Ring1B*^{fl^{ox}/fl^{ox}} (control) or *Ring1B*^{fl^{ox}/fl^{ox}};ERT2-Cre (*Ring1B* KO) mice were cultured in suspension for 3 days with 4-OHT and transfected with control siRNA oligonucleotide and two siRNA oligonucleotides against *Fezf2* (siFezf2 #1 and siFezf2 #2). Cells were then cultured for an additional 3 days without FGF2 or EGF. The level of *Fezf2* mRNA was determined (H). The percentage of CTIP2-positive neurons among βIII-tubulin-positive cells was determined (I). Data are means±s.e.m. of values from 12 samples. ***P*<0.01 (control versus *Ring1B* KO mice), #*P*<0.05, ###*P*<0.01 (control siRNA versus *Fezf2* siRNA oligo), n.s., not significant.

but is indispensable for its function in promoting the developmental changes of NPC fate.

An issue that has been questioned with regard to the subtype specification of neocortical neurons is whether these subtypes are specified within NPCs or at postmitotic stages. Microculture (Shen et al., 2006) and heterochronic transplant experiments (McConnell and Kaznowski, 1991) have suggested that neocortical neuronal subtypes are, at least in part, determined within NPCs in the VZ (independent of extracellular signaling). Our findings presented here are consistent with this notion, as *Ring1B* complexes modulate the

SCPN identity within NPCs: H3K27me3 and *Ring1B* accumulated at the *Fezf2* locus in a developmental stage-dependent manner in NPCs, and *Ring1B* deletion derepressed the *Fezf2* locus in the late-stage NPCs. Importantly, *Ring1B* deletion using the Nestin-Cre driver in NPCs prolonged the production of CTIP2⁺ neurons, but deletion in postmitotic neurons, using the NEX-Cre driver, did not increase the number of CTIP2⁺ neurons. Therefore, *Ring1B* does not seem to play a role in this subtype specification in postmitotic neurons. Although our results support a model in which NPC-intrinsic mechanisms are important for subtype specification, it is possible that further

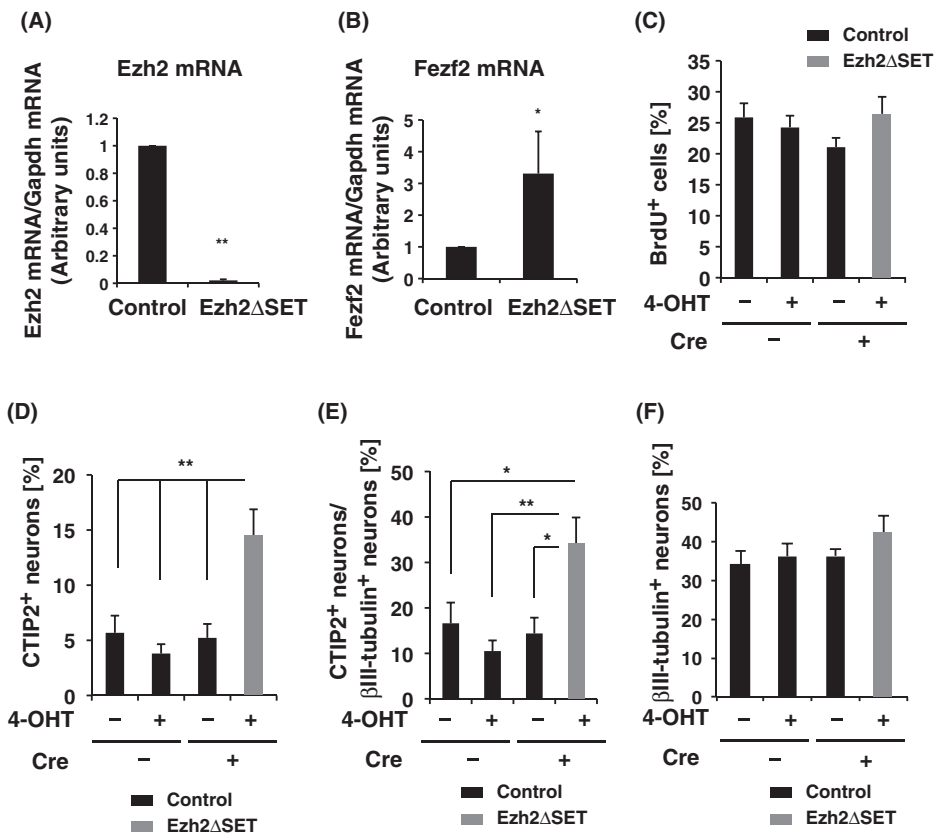


Fig. 7. Deleting the SET domain of *Ezh2* increases the amount of *Fezf2* mRNA and the percentage of CTIP2-positive neurons *in vitro*. (A,B) The methyltransferase activity of *Ezh2* is necessary for the repression of *Fezf2* expression *in vitro*. NPCs isolated from *Ezh2ΔSET^{fllox/fllox}*;ERT2-Cre mice at 12.5 dpc were cultured as described in Fig. 6A. The amount of mRNA indicated was measured by using RT-qPCR. Data are means+s.d. of values from three experiments. (C) Deleting the SET domain of *Ezh2* did not affect cell proliferation *in vitro*. NPCs isolated from *Ezh2ΔSET^{fllox/fllox}*;ERT2-Cre mice at 12.5 dpc were treated as described in Fig. 6E. Data are means+s.e.m. of values from six samples. Analysis of variance (ANOVA) was performed. (D,E) *Ezh2* regulates the production of CTIP2-positive (CTIP2⁺) neurons *in vitro*. NPCs isolated from *Ezh2ΔSET^{fllox/fllox}*;ERT2-Cre mice at 12.5 dpc were treated as described in Fig. 6F. The percentage of CTIP2⁺ cells (D) and CTIP2⁺ cells among βIII-tubulin-positive (βIII-tubulin⁺) cells (E) were determined. Data are means+s.e.m. of values from six samples. Tukey–Kramer test, * $P < 0.05$, ** $P < 0.01$. (F) Deleting the SET domain of *Ezh2* did not affect differentiation *in vitro*. NPCs isolated from *Ezh2ΔSET^{fllox/fllox}*;ERT2-Cre mice at 12.5 dpc were treated as described in D. Data are means+s.e.m. of values from six samples. ANOVA was performed.

specification occurs at postmitotic stages, perhaps through extrinsic signaling. Previous studies have indicated that the laminar and areal identities of some neocortical neuronal subtypes, including those determining axonal and/or dendritic patterns, are also affected after neuronal differentiation through interactions with various cues in the cortical plate. Indeed, some transcription factors (e.g. SOX5, Tbr1 and Bhlhb5) that are expressed only in postmitotic neurons have been shown to modulate the laminar and areal identities of neuronal subtypes (Bedogni et al., 2010; Fishell and Hanashima, 2008; Han et al., 2011; Joshi et al., 2008; Lai et al., 2008). It is therefore plausible that neuronal subtype identities are specified at multiple steps before and after exiting the cell cycle.

MATERIALS AND METHODS

Animals

A Ring1B^{fllox/fllox} mouse (Cales et al., 2008; Endoh et al., 2008) was crossed with either a ROSA26::ERT2-Cre mouse (ERT2-Cre driven by the endogenous *Rosa26* promoter), a NesCreERT2 mouse (ERT2-Cre driven by the Nestin enhancer) (Imayoshi et al., 2006), a NEX-Cre mouse (Goebbels et al., 2006) or an Emx1-CreERT2 mouse (Kessaris et al., 2006). An *Ezh2ΔSET^{fllox/fllox}* mouse (Hirabayashi et al., 2009) was crossed with a ROSA26::ERT2-Cre mouse.

Tamoxifen (Sigma) was dissolved in sunflower oil (Nacalai) at a concentration of 10 mg/ml. To induce ERT2-Cre activity, pregnant mice were injected intraperitoneally with 150 μl of tamoxifen solution.

All mice were maintained according to the protocol approved by the Animal Care and Use Committee of the University of Tokyo.

FACS

Cell suspensions were obtained from dissociated neocortices and stained with a Phycoerythrin (PE)-conjugated antibody against CD133 (BioLegend). Cell sorting was performed using a FACS Aria cell sorter (Becton Dickinson). Analysis was performed using the FACS Canto flow cytometer (Becton Dickinson).

Immunohistochemistry

Immunohistochemistry (IHC) was performed as previously described (Hirabayashi et al., 2004). Briefly, brains were fixed for 2 hours in 4% PFA in PBS, incubated overnight at 4°C with 30% (w/v) sucrose in PBS, embedded in OCT compound (Sakura Finetek) and cut with a cryostat to yield 10 or 12 μm-thick sections. Sections were blocked in 0.1% Triton X-100 and 2% donkey serum in Tris-buffered saline for 1 hour at room temperature. Primary antibodies diluted in blocking solution were added before an overnight incubation at 4°C. Then, sections were incubated with secondary antibodies diluted in blocking solution for 40 minutes at room temperature, and mounted in Mowiol (Calbiochem). Images were analyzed using a laser scanning confocal microscope (LSM510, Carl Zeiss; TSC-SP5, Leica) and processed with Photoshop CS software (Adobe). For the primary antibodies and dilutions, see supplementary materials.

EdU or BrdU birthdating

BrdU (100 mg/kg; Sigma) or EdU (50 mg/kg; Invitrogen) was injected into pregnant mice at 14.5 dpc (1 dpc was defined as 12 h after detection of the vaginal plug). Pups were collected at 18 dpc or P2, and BrdU- and EdU-positive cells were determined by immunohistochemistry. EdU was detected using Click-it kit (Invitrogen).

Reverse transcription quantitative PCR

For reverse transcription quantitative PCR (RT-qPCR), total RNA was obtained from NPCs using RNAiso (Takara) following the instructions of the manufacturer. Reverse transcription (RT) was performed using 2–5 μg of total RNA, oligo(dT)12–18 (Invitrogen) primers and ReverTra Ace (TOYOBO). The resulting cDNA was subjected to real-time PCR in a Roche LightCycler with SYBR Premix Ex Taq (Takara; Roche). The primers used are given in the supplementary materials.

Chromatin immunoprecipitation assay

For H3K27me3 chromatin immunoprecipitation (ChIP), cells were first fixed in 0.5% PFA, placed in a lysis buffer, and then sonicated to shear genomic chromatin into DNA fragments. The lysate was incubated with

Dynabeads Protein A (Invitrogen), after which the beads were removed and the lysate was incubated with antibody and protein A beads. The beads were then isolated and washed with Wash buffer and with TE buffer. After elution of immune complexes, the proteins were then eliminated by digestion with proteinase K.

For Ring1B ChIP, cells were first fixed in 1% formaldehyde and then placed in a swelling buffer. After removing the swelling buffer, they were suspended in RIPA buffer and sonicated to shear genomic chromatin into DNA fragments. The lysate was incubated with Dynabeads Protein A (Invitrogen), after which the beads were removed and the lysate was incubated with antibody and protein A beads. The beads were then isolated and rinsed with RIPA buffer, then washed with RIPA buffer, with RIPA + 500 mM NaCl buffer, with LiCl wash buffer and with TE buffer. After elution of immune complexes, the proteins were eliminated by digestion with proteinase K.

The DNA was then extracted with PCI (phenol/chlorophorm/isoamylalcohol) and EtOH, after which it was rinsed with 70% EtOH and suspended in water. The eluted DNA was subjected to real-time PCR in a Roche Light-cycler using Thunderbird SYBR qPCR mix (TOYOBO). Details of the antibodies, primers and buffer compositions are given in the supplementary material methods.

Retrograde labeling

SCPNs were labeled in a retrograde manner at P1 by injection of CTB555 (5 mg/ml in PBS, Invitrogen) into the pons-midbrain junction of control (Ring1B^{flox/flox}) or Ring1B^{flox/flox};NesCreERT2 pups. At 1.5 days after the injection, perfusion was performed.

Primary NPC culture

Primary NPCs were prepared from the dorsal cerebral cortex of ICR mouse embryos at 11 dpc or Ring1B^{flox/flox};ROSACreERT mouse embryos as previously described (Hirabayashi et al., 2009).

BrdU proliferation assay

Cells were labeled with BrdU (20 µg/ml) for 30 min. BrdU-positive cells were quantified using immunocytochemistry.

Immunocytochemistry

Cells were fixed with 4% paraformaldehyde in PBS, permeabilized with 0.5% Triton X-100 in 3% BSA in PBS for 30 min, incubated with primary antibodies diluted in 3% BSA in PBS overnight at 4°C and then with secondary antibodies for 40 min at room temperature and mounted in Mowiol (Calbiochem). For the primary antibodies and dilutions, see supplementary materials.

siRNA

siRNAs were introduced into 3-DIV NPCs collected from Ring1B^{flox/flox};ROSACreERT mice at 14 dpc by using Amaxa (Lonza). For the siRNA oligonucleotides used, see supplementary materials.

Statistical analysis

All data are representative of results obtained from at least three independent experiments. Statistical significance was determined by two-tailed Student's *t*-test, unless otherwise indicated.

Acknowledgements

We thank H. Maruoka, T. Hosoya, J. Macklis, K. Touhara, Y. Ueta and Y. Kawaguchi for instruction on retrograde labeling; R. Kageyama for NesCreERT2 mice; K. A. Nave and N. Tamamaki for NEX-Cre mice; N. Kessaris for Emx1-CreERT2 mice; J. Takeuchi, Y. Kishi and Ms H. Sugizaki for FACS analysis.

Competing interests

The authors declare no competing financial interests.

Author contributions

N.M. designed and performed experiments and data analysis and prepared the manuscript with Y.H. and Y.G. Y.H. conceived and supervised the entire project with Y.G. K.T. performed experiments and edited the manuscript. J.S. and H.K. generated the *Ezh2* dSET mice. M.V. and H.K. generated the Ring1B^{flox} mice.

Funding

N.M.-S. was a research fellow of the Japan Society for the Promotion of Science (JSPS). This work was supported by Core Research for Evolutionary Science and Technology (CREST) of the Japan Science and Technology Agency; and Grant-in-Aid for Scientific Research on Innovative Areas 'Neural Diversity and Neocortical Organization' for Scientific Research (A), for JSPS fellows from JSPS; and the Global Center of Excellence (COE) Program (Integrative Life Science Based on the Study of Biosignaling Mechanisms) from Japan's Ministry of Education, Culture, Sports, Science and Technology (MEXT, Japan).

Supplementary material

Supplementary material available online at <http://dev.biologists.org/lookup/suppl/doi:10.1242/dev.112276/-DC1>

References

- Alcama, E. A., Chirivella, L., Dautzenberg, M., Dobrova, G., Fariñas, I., Grosschedl, R. and McConnell, S. K. (2008). *Satb2* regulates callosal projection neuron identity in the developing cerebral cortex. *Neuron* **57**, 364-377.
- Aldiri, I. and Vetter, M. L. (2012). PRC2 during vertebrate organogenesis: a complex in transition. *Dev. Biol.* **367**, 91-99.
- Arlotta, P., Molyneaux, B. J., Chen, J., Inoue, J., Kominami, R. and Macklis, J. D. (2005). Neuronal subtype-specific genes that control corticospinal motor neuron development in vivo. *Neuron* **45**, 207-221.
- Ayala, R., Shu, T. and Tsai, L.-H. (2007). Trekking across the brain: the journey of neuronal migration. *Cell* **128**, 29-43.
- Bedogni, F., Hodge, R. D., Elsen, G. E., Nelson, B. R., Daza, R. A. M., Beyer, R. P., Bammler, T. K., Rubenstein, J. L. R. and Hevner, R. F. (2010). *Tbr1* regulates regional and laminar identity of postmitotic neurons in developing neocortex. *Proc. Natl. Acad. Sci. USA* **107**, 13129-13134.
- Bernstein, B. E., Meissner, A. and Lander, E. S. (2007). The mammalian epigenome. *Cell* **128**, 669-681.
- Britanova, O., de Juan Romero, C., Cheung, A., Kwan, K. Y., Schwark, M., Gyorgy, A., Vogel, T., Akopov, S., Mitkovski, M., Agoston, D. et al. (2008). *Satb2* is a postmitotic determinant for upper-layer neuron specification in the neocortex. *Neuron* **57**, 378-392.
- Cabianca, D. S., Casa, V., Bodega, B., Xynos, A., Ginelli, E., Tanaka, Y. and Gabellini, D. (2012). A long ncRNA links copy number variation to a polycomb/trithorax epigenetic switch in FSHD muscular dystrophy. *Cell* **149**, 819-831.
- Cales, C., Roman-Trufero, M., Pavon, L., Serrano, I., Melgar, T., Endoh, M., Perez, C., Koseki, H. and Vidal, M. (2008). Inactivation of the Polycomb group protein Ring1B unveils an antiproliferative role in hematopoietic cell expansion and cooperation with tumorigenesis associated to *Ink4a* deletion. *Mol. Cell. Biol.* **28**, 1018-1028.
- Cao, R. and Zhang, Y. (2004). The functions of E(Z)/EZH2-mediated methylation of lysine 27 in histone H3. *Curr. Opin. Genet. Dev.* **14**, 155-164.
- Chen, B., Schaevitz, L. R. and McConnell, S. K. (2005a). *Fezl* regulates the differentiation and axon targeting of layer 5 subcortical projection neurons in cerebral cortex. *Proc. Natl. Acad. Sci. USA* **102**, 17184-17189.
- Chen, J.-G., Rasin, M.-R., Kwan, K. Y. and Sestan, N. (2005b). *Zfp312* is required for subcortical axonal projections and dendritic morphology of deep-layer pyramidal neurons of the cerebral cortex. *Proc. Natl. Acad. Sci. USA* **102**, 17792-17797.
- De la Rossa, A., Bellone, C., Golding, B., Vitali, I., Moss, J., Toni, N., Lüscher, C. and Jabaudon, D. (2013). In vivo reprogramming of circuit connectivity in postmitotic neocortical neurons. *Nat. Neurosci.* **16**, 193-200.
- de Napolés, M., Mermoud, J. E., Wakao, R., Tang, Y. A., Endoh, M., Appanah, R., Nesterova, T. B., Silva, J., Otte, A. P., Vidal, M. et al. (2004). Polycomb group proteins Ring1A/B link ubiquitylation of histone H2A to heritable gene silencing and X inactivation. *Dev. Cell* **7**, 663-676.
- Desai, A. R. and McConnell, S. K. (2000). Progressive restriction in fate potential by neural progenitors during cerebral cortical development. *Development* **127**, 2863-2872.
- Eiraku, M., Watanabe, K., Matsuo-Takasaki, M., Kawada, M., Yonemura, S., Matsumura, M., Wataya, T., Nishiyama, A., Muguruma, K. and Sasai, Y. (2008). Self-organized formation of polarized cortical tissues from ESCs and its active manipulation by extrinsic signals. *Cell Stem Cell* **3**, 519-532.
- Endoh, M., Endo, T. A., Endoh, T., Fujimura, Y.-i., Ohara, O., Toyoda, T., Otte, A. P., Okano, M., Brockdorff, N., Vidal, M. et al. (2008). Polycomb group proteins Ring1A/B are functionally linked to the core transcriptional regulatory circuitry to maintain ES cell identity. *Development* **135**, 1513-1524.
- Fasano, C. A., Dimos, J. T., Ivanova, N. B., Lowry, N., Lemischka, I. R. and Temple, S. (2007). shRNA knockdown of *Bmi-1* reveals a critical role for p21-rb pathway in NSC self-renewal during development. *Cell Stem Cell* **1**, 87-99.
- Fasano, C. A., Phoenix, T. N., Kokovay, E., Lowry, N., Elkabetz, Y., Dimos, J. T., Lemischka, I. R., Studer, L. and Temple, S. (2009). *Bmi-1* cooperates with *Foxg1* to maintain neural stem cell self-renewal in the forebrain. *Genes Dev.* **23**, 561-574.
- Fishell, G. and Hanashima, C. (2008). Pyramidal neurons grow up and change their mind. *Neuron* **57**, 333-338.

- Franco, S. J., Gil-Sanz, C., Martinez-Garay, I., Espinosa, A., Harkins-Perry, S. R., Ramos, C. and Muller, U. (2012). Fate-restricted neural progenitors in the mammalian cerebral cortex. *Science* **337**, 746-749.
- Gao, Z. H., Zhang, J., Bonasio, R., Strino, F., Sawai, A., Parisi, F., Kluger, Y. and Reinberg, D. (2012). PCGF Homologs, CBX Proteins, and RYBP Define Functionally Distinct PRC1 Family Complexes. *Mol. Cell* **45**, 344-356.
- Gaspard, N., Bouschet, T., Hourez, R., Dimidschstein, J., Naeije, G., van den Aemele, J., Espuny-Camacho, I., Herpoel, A., Passante, L., Schiffmann, S. N. et al. (2008). An intrinsic mechanism of corticogenesis from embryonic stem cells. *Nature* **455**, 351-357.
- Goebbels, S., Bormuth, I., Bode, U., Hermanson, O., Schwab, M. H. and Nave, K.-A. (2006). Genetic targeting of principal neurons in neocortex and hippocampus of NEX-Cre mice. *Genesis* **44**, 611-621.
- Guo, C., Eckler, M. J., McKenna, W. L., McKinsey, G. L., Rubenstein, J. L. R. and Chen, B. (2013). Fezf2 expression identifies a multipotent progenitor for neocortical projection neurons, astrocytes, and oligodendrocytes. *Neuron* **80**, 1167-1174.
- Gutman, M. and Rinn, J. L. (2012). Modular regulatory principles of large non-coding RNAs. *Nature* **482**, 339-346.
- Han, W., Kwan, K. Y., Shim, S., Lam, M. M. S., Shin, Y., Xu, X., Zhu, Y., Li, M. and Sestan, N. (2011). TBR1 directly represses Fezf2 to control the laminar origin and development of the corticospinal tract. *Proc. Natl. Acad. Sci. USA* **108**, 3041-3046.
- Hanashima, C., Li, S. C., Shen, L. J., Lai, E. S. and Fishell, G. (2004). Foxg1 suppresses early cortical cell fate. *Science* **303**, 56-59.
- Hevner, R. F., Daza, R. A. M., Rubenstein, J. L. R., Stunnenberg, H., Olavarria, J. F. and Englund, C. (2003). Beyond laminar fate: toward a molecular classification of cortical projection/pyramidal neurons. *Dev. Neurosci.* **25**, 139-151.
- Hirabayashi, Y., Itoh, Y., Tabata, N., Nakajima, K., Akiyama, T., Masuyama, N. and Gotoh, Y. (2004). The Wnt/beta-catenin pathway directs neuronal differentiation of cortical neural precursor cells. *Development* **131**, 2791-2801.
- Hirabayashi, Y., Suzuki, N., Tsuboi, M., Endo, T. A., Toyoda, T., Shinga, J., Koseki, H., Vidal, M. and Gotoh, Y. (2009). Polycomb limits the neurogenic competence of neural precursor cells to promote astrogenic fate transition. *Neuron* **63**, 600-613.
- Hirata, T., Suda, Y., Nakao, K., Narimatsu, M., Hirano, T. and Hibi, M. (2004). Zinc finger gene fez-like functions in the formation of subplate neurons and thalamocortical axons. *Dev. Dyn.* **230**, 546-556.
- Imayoshi, I., Ohtsuka, T., Metzger, D., Chambon, P. and Kageyama, R. (2006). Temporal regulation of Cre recombinase activity in neural stem cells. *Genesis* **44**, 233-238.
- Joshi, P. S., Molyneaux, B. J., Feng, L., Xie, X., Macklis, J. D. and Gan, L. (2008). Bhlhb5 regulates the postmitotic acquisition of area identities in layers II-V of the developing neocortex. *Neuron* **60**, 258-272.
- Kessarlis, N., Fogarty, M., Iannarelli, P., Grist, M., Wegner, M. and Richardson, W. D. (2006). Competing waves of oligodendrocytes in the forebrain and postnatal elimination of an embryonic lineage. *Nat. Neurosci.* **9**, 173-179.
- Kohwi, M. and Doe, C. Q. (2013). Temporal fate specification and neural progenitor competence during development. *Nat. Rev. Neurosci.* **14**, 823-838.
- Kriegstein, A. R. and Noctor, S. C. (2004). Patterns of neuronal migration in the embryonic cortex. *Trends Neurosci.* **27**, 392-399.
- Kwan, K. Y., Sestan, N. and Anton, E. S. (2012). Transcriptional co-regulation of neuronal migration and laminar identity in the neocortex. *Development* **139**, 1535-1546.
- Lai, T., Jabaudon, D., Molyneaux, B. J., Azim, E., Arlotta, P., Menezes, J. R. L. and Macklis, J. D. (2008). SOX5 controls the sequential generation of distinct corticofugal neuron subtypes. *Neuron* **57**, 232-247.
- Leeb, M., Pasini, D., Novatchkova, M., Jaritz, M., Helin, K. and Wutz, A. (2010). Polycomb complexes act redundantly to repress genomic repeats and genes. *Genes Dev.* **24**, 265-276.
- Leone, D. P., Srinivasan, K., Chen, B., Alcamo, E. and McConnell, S. K. (2008). The determination of projection neuron identity in the developing cerebral cortex. *Curr. Opin. Neurobiol.* **18**, 28-35.
- Luis, N. M., Morey, L., Di Croce, L. and Benitah, S. A. (2012). Polycomb in Stem Cells: PRC1 Branches Out. *Cell Stem Cell* **11**, 16-21.
- Margueron, R. and Reinberg, D. (2011). The Polycomb complex PRC2 and its mark in life. *Nature* **469**, 343-349.
- Maruoka, H., Kubota, K., Kurokawa, R., Tsuruno, S. and Hosoya, T. (2011). Periodic organization of a major subtype of pyramidal neurons in neocortical layer V. *J. Neurosci.* **31**, 18522-18542.
- McConnell, S. K. and Kaznowski, C. E. (1991). Cell cycle dependence of laminar determination in developing neocortex. *Science* **254**, 282-285.
- Molyneaux, B. J., Arlotta, P., Hirata, T., Hibi, M. and Macklis, J. D. (2005). Fezl is required for the birth and specification of corticospinal motor neurons. *Neuron* **47**, 817-831.
- Molyneaux, B. J., Arlotta, P., Menezes, J. R. L. and Macklis, J. D. (2007). Neuronal subtype specification in the cerebral cortex. *Nat. Rev. Neurosci.* **8**, 427-437.
- Naka, H., Nakamura, S., Shimazaki, T. and Okano, H. (2008). Requirement for COUP-TFI and II in the temporal specification of neural stem cells in CNS development. *Nat. Neurosci.* **11**, 1014-1023.
- Noctor, S. C., Flint, A. C., Weissman, T. A., Dammerman, R. S. and Kriegstein, A. R. (2001). Neurons derived from radial glial cells establish radial units in neocortex. *Nature* **409**, 714-720.
- Onoguchi, M., Hirabayashi, Y., Koseki, H. and Gotoh, Y. (2012). A noncoding RNA regulates the neurogenin1 gene locus during mouse neocortical development. *Proc. Natl. Acad. Sci. USA* **109**, 16939-16944.
- O'Leary, D. D. M. and Koester, S. E. (1993). Development of projection neuron types, axon pathways, and patterned connections of the mammalian cortex. *Neuron* **10**, 991-1006.
- Pasinelli, P. and Brown, R. H. (2006). Molecular biology of amyotrophic lateral sclerosis: insights from genetics. *Nat. Rev. Neurosci.* **7**, 710-723.
- Pereira, J. D., Sansom, S. N., Smith, J., Dobenecker, M.-W., Tarakhovskiy, A. and Livesey, F. J. (2010). Ezh2, the histone methyltransferase of PRC2, regulates the balance between self-renewal and differentiation in the cerebral cortex. *Proc. Natl. Acad. Sci. USA* **107**, 15957-15962.
- Polleux, F., Dehay, C. and Kennedy, H. (1997). The timetable of laminar neurogenesis contributes to the specification of cortical areas in mouse isocortex. *J. Comp. Neurol.* **385**, 95-116.
- Qian, X., Shen, Q., Goderie, S. K., He, W., Capela, A., Davis, A. A. and Temple, S. (2000). Timing of CNS cell generation: a programmed sequence of neuron and glial cell production from isolated murine cortical stem cells. *Neuron* **28**, 69-80.
- Rouaux, C. and Arlotta, P. (2013). Direct lineage reprogramming of post-mitotic callosal neurons into corticofugal neurons in vivo. *Nat. Cell Biol.* **15**, 214-221.
- Sauvageau, M. and Sauvageau, G. (2010). Polycomb group proteins: multi-faceted regulators of somatic stem cells and cancer. *Cell Stem Cell* **7**, 299-313.
- Schoeffner, S., Sengupta, A. K., Kubicek, S., Mechtler, K., Spahn, L., Koseki, H. H., Jenwein, T. and Wutz, A. (2006). Recruitment of PRC1 function at the initiation of X inactivation independent of PRC2 and silencing. *EMBO J.* **25**, 3110-3122.
- Schwartz, Y. B. and Pirrotta, V. (2007). Polycomb silencing mechanisms and the management of genomic programmes. *Nat. Rev. Genet.* **8**, 9-22.
- Shen, Q., Wang, Y., Dimos, J. T., Fasano, C. A., Phoenix, T. N., Lemischka, I. R., Ivanova, N. B., Stifani, S., Morrissey, E. E. and Temple, S. (2006). The timing of cortical neurogenesis is encoded within lineages of individual progenitor cells. *Nat. Neurosci.* **9**, 743-751.
- Sing, A., Pannell, D., Karaiskakis, A., Sturgeon, K., Djabali, M., Ellis, J., Lipshitz, H. D. and Cordes, S. P. (2009). A vertebrate polycomb response element governs segmentation of the posterior hindbrain. *Cell* **138**, 885-897.
- Sparmann, A. and van Lohuizen, M. (2006). Polycomb silencers control cell fate, development and cancer. *Nat. Rev. Cancer* **6**, 846-856.
- Sparmann, A., Xie, Y., Verhoeven, E., Vermeulen, M., Lancini, C., Gargiulo, G., Hulsman, D., Mann, M., Knoblich, J. A. and van Lohuizen, M. (2013). The chromodomain helicase Chd4 is required for Polycomb-mediated inhibition of astroglial differentiation. *EMBO J.* **32**, 1598-1612.
- Tavares, L., Dimitrova, E., Oxley, D., Webster, J., Demmers, J., Bezstarosti, K., Taylor, S., Ura, H., Koide, H. et al. (2012). RYBP-PRC1 Complexes Mediate H2A Ubiquitylation at Polycomb Target Sites Independently of PRC2 and H3K27me3. *Cell* **148**, 664-678.
- Testa, G. (2011). The time of timing: how Polycomb proteins regulate neurogenesis. *Bioessays* **33**, 519-528.
- Touma, J. J., Weckerle, F. F. and Cleary, M. D. (2012). Drosophila Polycomb complexes restrict neuroblast competence to generate motoneurons. *Development* **139**, 657-666.
- Woo, C. J., Kharchenko, P. V., Daheron, L., Park, P. J. and Kingston, R. E. (2010). A region of the human HOXD cluster that confers polycomb-group responsiveness. *Cell* **140**, 99-110.
- Wu, S.-X., Goebbels, S., Nakamura, K., Kometani, K., Minato, N., Kaneko, T., Nave, K.-A. and Tamamaki, N. (2005). Pyramidal neurons of upper cortical layers generated by NEX-positive progenitor cells in the subventricular zone. *Proc. Natl. Acad. Sci. USA* **102**, 17172-17177.
- Zhao, J., Ohsumi, T. K., Kung, J. T., Ogawa, Y., Grau, D. J., Sarma, K., Song, J. J., Kingston, R. E., Borowsky, M. and Lee, J. T. (2010). Genome-wide identification of polycomb-associated RNAs by RIP-seq. *Mol. Cell* **40**, 939-953.

Supplementary methods

Immunohistochemistry (IHC)

Brains were fixed for 2 hours in 4% PFA/PBS, incubated overnight at 4°C with 30% (w/v) sucrose in PBS, embedded in OCT compound (Sakura Finetek), and cut with a cryostat to yield 10 or 12 µm-thick sections. Sections were blocked in 0.1% Triton X-100 and 2% donkey serum in Tris-buffered saline (140 mM NaCl, 25 mM Tris-HCl, pH 7.5) for 1 hour at room temperature. Primary antibodies diluted in blocking solution were added before an overnight incubation at 4°C. Then, sections were incubated with secondary antibodies diluted in blocking solution for 40 minutes at room temperature, and mounted in Mowiol (Calbiochem). Images were analyzed using a laser scanning confocal microscope (LSM510, Carl Zeiss; TSC-SP5, Leica). Images were processed with Photoshop CS software (Adobe). Primary antibodies and dilutions used are as follows: rat anti-CTIP2, 1:2000 (Abcam); mouse anti-Ring1B, 1:200 (MBL); rat anti-BrdU, 1:200 (Abcam); mouse anti-BrdU, 1:500 (BD); rabbit anti-Cux1, 1:200 (SantaCruz); rabbit anti-Tbr1, 1:1000 (Abcam); rabbit anti-Sox5, 1:1000 (Abcam); rabbit anti-Pax6, 1:200 (Millipore); rabbit anti-Tbr2, 1:1000 (Abcam); rabbit anti-pH3,

1:200 (Cell Signaling); mouse anti-Satb2, 1:200 (Abcam); mouse anti- β III-tubulin, 1:1000 (Covance); rabbit anti-Ki67, 1:200 (Novocastra).

RT-qPCR

Total RNA was obtained from NPCs using RNAiso (Takara) following the instructions of the manufacturer. Reverse transcription (RT) was performed with 2-5 μ g of total RNA, oligod(T)12-18 (Invitrogen) primers, and ReverTra Ace (TOYOBO). The resulting cDNA was subjected to real-time PCR in a Roche LightCycler with SYBR Premix Ex Taq (Takara; Roche). The amount of target mRNA was normalized relative to that of *Gapdh* mRNA. The primers used are as follows: *Fezf2*, sense 5'-

CTCTACTGACAGCAAACCCA-3' and antisense 5'-

CTTTGCACACAAACGGTCT-3'; *Gapdh*, sense 5'-TGGGTGTGAACCACGA-3' and

antisense 5'-AAGTTGTCATGGATGACCTT-3'; β III-tubulin, sense

5'-ACACAGACGAGACCTACT-3' and antisense 5'-GCAGACACAAGGTGGTT-3';

Ring1B, sense 5'-AGTTACAACGAACACCTCAG-3' and antisense 5'-

TCCAAACAAATTGGGCACAT-3'; *Pax6*, sense

5'-CGGAGGGAGTAAGCCAAGAG-3' and antisense

5'-TCTGTCTCGGATTTCCCAAG-3'; Ezh2 (SET domain), sense

5'-TTTGCTAATCATTTCAGTAAATCCAAAC-3' and antisense

5'-GCAAAGATGCCTATCCTGTG-3'.

ChIP

For H3K27me3 ChIP, cells were first fixed in 0.5% PFA for 10 minutes at room temperature, put on ice in a Lysis buffer [1% SDS, 10 mM EDTA, 50 mM Tris-HCl (pH 8.1)] for 10 minutes, and then sonicated to shear genomic chromatin into DNA fragments. The lysate was incubated with Dynabeads Protein A (Invitrogen) for 1 hour at 4°C, after which the beads were removed and the lysate was incubated overnight at 4°C with antibody and protein A beads. The beads were then isolated and washed 8 times with Wash buffer [50 mM HEPES-KOH (pH7.6), 500 mM LiCl, 1 mM EDTA (pH8.0), 1% NP-40, 0.7% Na-Deoxycholate], and twice with TE buffer [10 mM TrisHCl (pH 8.0), 1 mM EDTA]. To elute immune complexes from the beads, the beads were incubated at 65°C for 15 minutes in a solution containing 10 mM Tris-HCl (pH

8.0), 5 mM EDTA, 300 mM NaCl, and 0.5% SDS. Then the beads were removed, and the eluate was incubated at 65°C overnight. The proteins then were eliminated by digestion with proteinase K at 55°C for 1 hour. The DNA was then extracted with PCI (phenol/chlorophorm/isoamylalcohol) and EtOH, after which it was rinsed with 70% EtOH and suspended in water. The eluted DNA was subjected to real-time PCR in a Roche Light- cycler using Thunderbird SYBR qPCR mix (TOYOBO).

For Ring1B ChIP, cells were first fixed in 1% formaldehyde for 10 minutes at room temperature and then put on ice in a swelling buffer [20 mM Hepes (pH 7.8), 1.5 mM MgCl₂, 10 mM KCl, 0.1% NP-40, 1 mM DTT] for 10 minutes. After removing the swelling buffer, they were suspended in RIPA buffer [10 mM Tris-HCl (pH 8.0), 1 mM EDTA, 140 mM NaCl, 1% Triton X-100, 0.1% SDS, 0.1% sodium deoxycholate (DOC)] and sonicated to shear genomic chromatin into DNA fragments. The lysate was incubated with Dynabeads Protein A (Invitrogen) for 1 hour at 4°C, after which the beads were removed and the lysate was incubated overnight at 4°C with antibody and protein A beads. The beads were then isolated and rinsed twice with RIPA buffer, then washed 6 times with RIPA buffer, twice with RIPA + 500 mM NaCl buffer, twice with

LiCl wash buffer [10 mM Tris-HCl (pH 8.0), 1 mM EDTA, 250 mM LiCl 0.5% NP-40, 0.5% DOC], and twice with TE buffer [10 mM TrisHCl (pH 8.0), 1 mM EDTA]. To elute immune complexes from the beads, the beads were incubated at 65°C for 15 minutes in a solution containing 10 mM Tris-HCl (pH8.0), 5 mM EDTA, 300 mM NaCl, and 0.5% SDS. Then the beads were removed, and the eluate was incubated at 65°C overnight. The proteins then were eliminated by digestion with proteinase K at 55°C for 1 hour. The DNA was then extracted with PCI (phenol/chlorophorm/isoamylalcohol) and EtOH, after which it was rinsed with 70% EtOH and suspended in water. The eluted DNA was subjected to real-time PCR in a Roche Light- cycler using Thunderbird SYBR qPCR mix (TOYOBO).

The sense and antisense primers used are as follows: Fezf2 promoter, sense 5'-ACATCCTAATGAGGTAATTATCATTG-3' and antisense 5'-ACCGTGCTAATAAACTGCC-3'; Gapdh promoter, sense 5'-TGCAGTCCGTATTTATAGGAACC-3' and antisense 5'-CTTGAGCTAGGACTGGATAAGCA-3'; Neurog1 promoter, sense 5'-CATTGTTGCGCGCCGTA-3' and antisense 5'-GCGATCAGATCAGCTCCT-3'.

siRNA

siRNA oligos used are as follows: control siRNA oligo, AAA UGC UUA GAU GAU

CAC UUA UCC C, Fezf2 siRNA oligo #1, MSS225765 (Invitrogen stealth siRNA),

siRNA oligo #2, MSS225766 (Invitrogen stealth siRNA).

Supplementary Figure S1. Ring1B deletion did not change the layer formation of

neocortex and excessively-produced-CTIP2⁺⁺ neurons did not express cux1.

Ring1B^{flox/flox} (Control; A, C) or Ring1B^{flox/flox};NesCreERT2 (Ring1B KO; B, D) mice

were treated with tamoxifen at 13.0 dpc. Then the embryos were fixed at P2.5 and

subjected to immunohistochemistry with the antibodies indicated. The primary

somatosensory areas are shown. Scale bar: 250 μm . Ring1B^{flox/flox} (Control; E, G, I) or

Ring1B^{flox/flox};NesCreERT2 (Ring1B KO; F, H, J) mice were treated with tamoxifen at

13.0 dpc. Then the embryos were fixed at P2.5 and subjected to immunohistochemistry

with the antibodies indicated. The primary somatosensory areas are shown. Scale bar:

100 μm .

Supplementary Figure S2. The distribution of Satb2⁺ cells and Cux1⁺ cells in the cortex. Ring1B^{flox/flox} (Control; black bars) or Ring1B^{flox/flox};NesCreERT2 (Ring1B KO; white bars) were treated with tamoxifen at 13.0 dpc. The pups' brains were fixed at P2.5 and subjected to immunohistochemistry with an anti-Satb2 antibody (A) and an anti-Cux1 antibody (B). The pups' brains were fixed at 18.5 dpc and subjected to immunohistochemistry with an anti-CTIP2 antibody (C), an anti-Satb2 antibody (D) and an anti-Cux1 antibody (E). Then cortical plate was equally divided into 10 bins positioned parallel to the brain surface. The number of each type of neurons in each bin was determined. Data are the means±s.d. of values of 16 corresponding areas of three control mice and 31 corresponding areas of five KO mice (A,B) or the means±s.d. of values of five hemispheres of three control mice and seven hemispheres of four KO mice (C-E). * $P < 0.05$, ** $P < 0.01$.

Supplementary Figure S3. Knockout of the *Ring1B* gene in postmitotic neurons

has little effect on the number of CTIP2⁺⁺ cells. The brains of control (A,C,E,G) and *Ring1B*^{flox/flox};NEX-Cre (B,D,F,H) mice were fixed at P0 (A-F) or P2 (G,H) and subjected to immunohistochemistry using the antibodies indicated. The number of CTIP2⁺⁺ or Cux1⁺ cells was determined (I- K). Data are the means±s.e.m. of values of eight corresponding areas of four control mice and six corresponding areas of three KO mouse (I, J). Data are the means±s.e.m. of values of six corresponding areas of four control mice and five corresponding areas of three KO mouse (K). Scale bar: 50 μm.

Supplementary Figure S4. Ring1B deletion did not significantly affect the number

of Pax6-positive neural precursor cells. Ring1B^{flox/flox} (Control, A) or

Ring1B^{flox/flox};NesCreERT2 (Ring1B KO NesCreER, B) mice were treated with

tamoxifen at 13.0 dpc. The pups' brains were fixed at P2 and subjected to

immunohistochemistry with an anti-Pax6 antibody. The number of Pax6⁺ cells was

determined (C). Ring1B^{flox/flox} (Control; D, G) or Ring1B^{flox/flox};Emx1-CreERT2

(Ring1B KO Emx1CreER; E, H) mice were treated with tamoxifen at 10 dpc. The pups'

brains were fixed at 12 dpc (D,E) or 17 dpc (G,H) and subjected to

immunohistochemistry with an anti-Pax6 antibody. The number of Pax6⁺ cells was

determined (F,I). Data are the means±s.d. of values of four corresponding areas of two

control mice and 4 corresponding areas of three KO mice (C), values of five

corresponding areas of one control mice and 22 corresponding areas of three KO mice

(F), values of ten corresponding areas of five control mice and six corresponding areas

of three KO mice (I). Scale bar: 50 μm.

Supplementary Figure S5. FACS gate information. The marked areas in each chart were collected from 14 dpc WT (A), 16 dpc WT (B), and 17 dpc Ring1B;NesCreERTs mice (C). (A,B) Cells were stained with anti-CD133 antibody (red histogram) or not stained (gray histogram) and CD133^{high} and CD133^{mid} (the fractions indicated by the black horizontal lines) were obtained by FACS. (D,E) CD133^{high} and CD133^{mid} cells (each black horizontal line, respectively) were obtained from cells isolated from control (D) and Ring1B KO (E) mouse embryos by FACS at 17 dpc. Cells were stained with anti-CD133 antibody (red histogram) or not stained (gray histogram).

Supplementary Figure S6. The level of Ring1B mRNA did not change between 14

dpc and 16 dpc. The amount of *Ring1B* mRNA in CD133^{high} NPCs of 14 dpc and 16

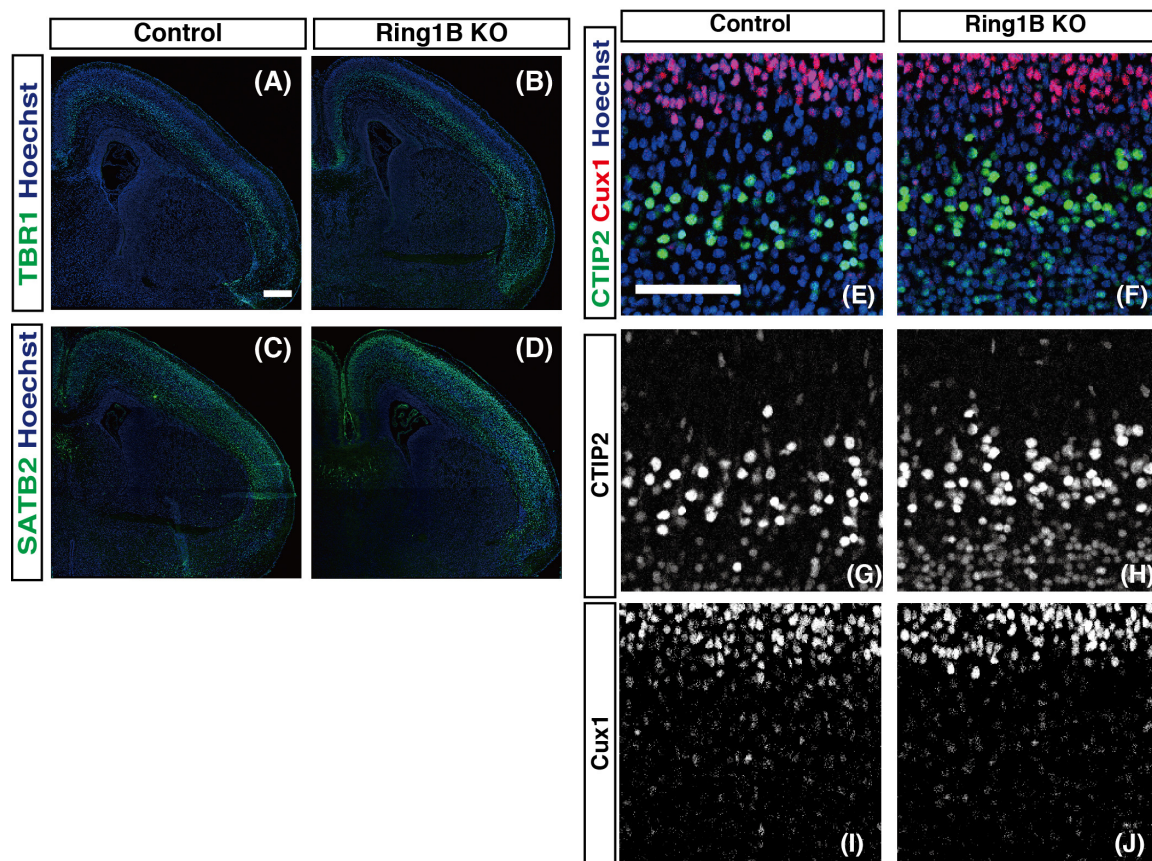
dpc was assessed using quantitative PCR. Data are means±s.e.m. of values from four

experiments.

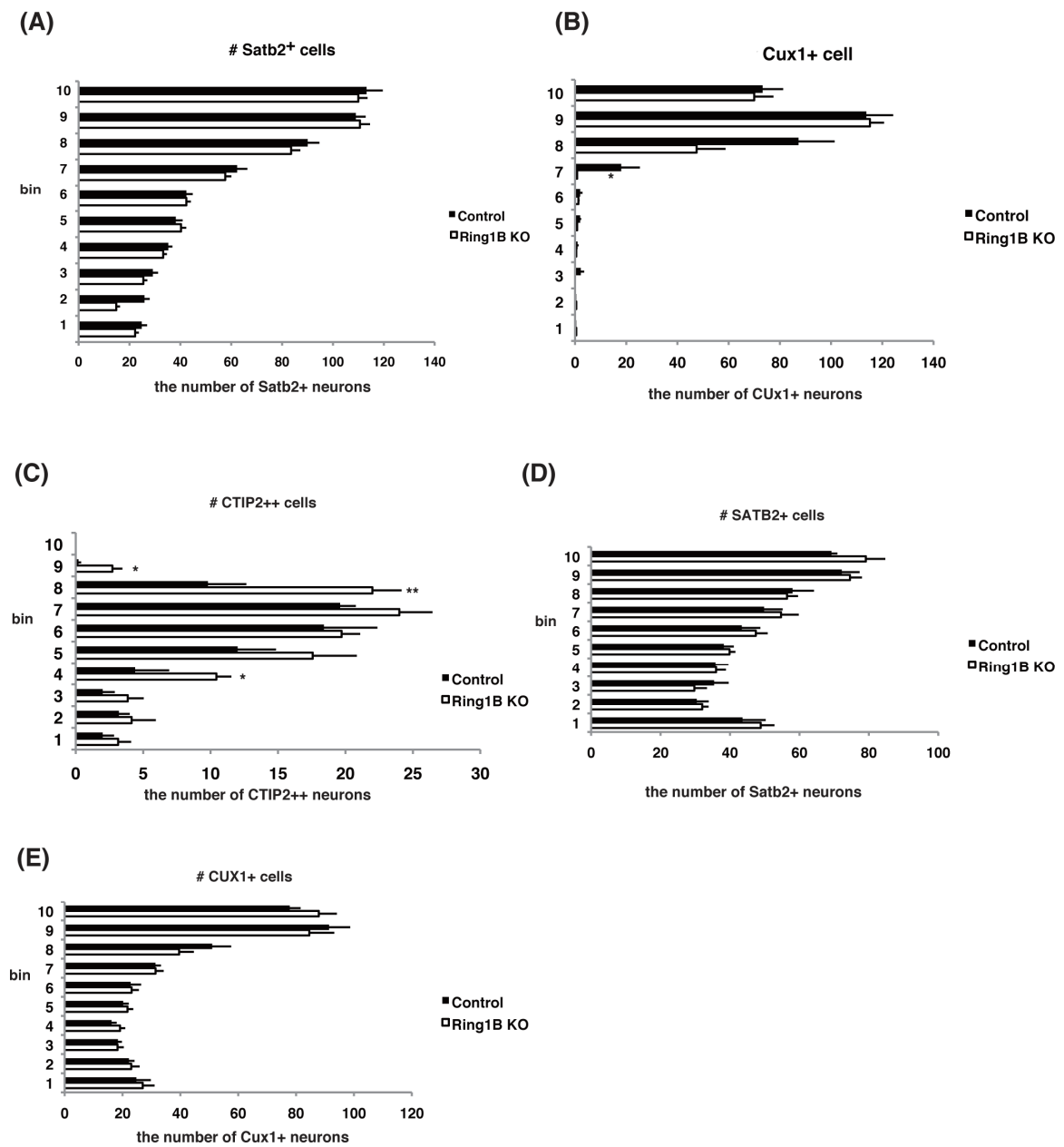
Supplementary Figure S7. The level of H3K27me3 at the *Fezf2* promoter and *Neurog1* promoter increased in the late neurogenic phase. The amount of H3K27me3 at the *Neurog1* promoter was assessed using ChIP and quantitative PCR. The neocortical ventricular zone/subventricular sections of 14 dpc, 16 dpc, or 19 dpc were manually isolated, and the chromatin complex from each stage was immunoprecipitated with anti-trimethylated K27 histoneH3. The immunoprecipitates were subjected to PCR amplification of the promoter region of each gene. The level of H3K27me3 at the *Fezf2* promoter increased between 14 dpc and 16 dpc, whereas the level at the *Gapdh* promoter remained constant. The level *Neurog1* promoter increased gradually during the neurogenic phase. Data are means \pm s.e.m. of values from three samples. ** $P < 0.01$.

Supplementary Figure S8. Fezf2 expression was induced in differentiating NPCs in the early stage of neurogenic phase and it was not in the late stage. Proposed model of the role of PcG proteins in terminating SCPN production.

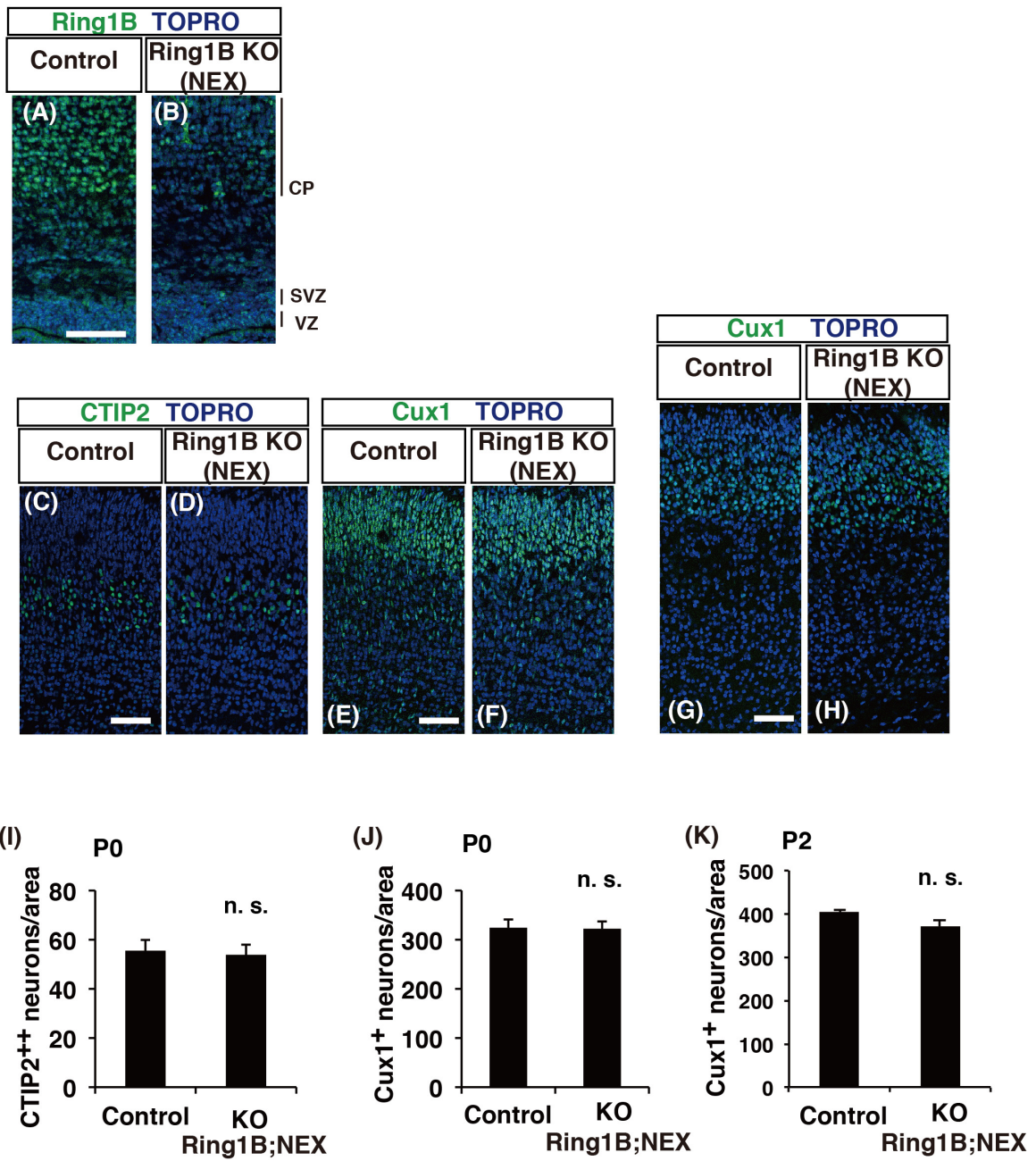
Supplemental Figure 1



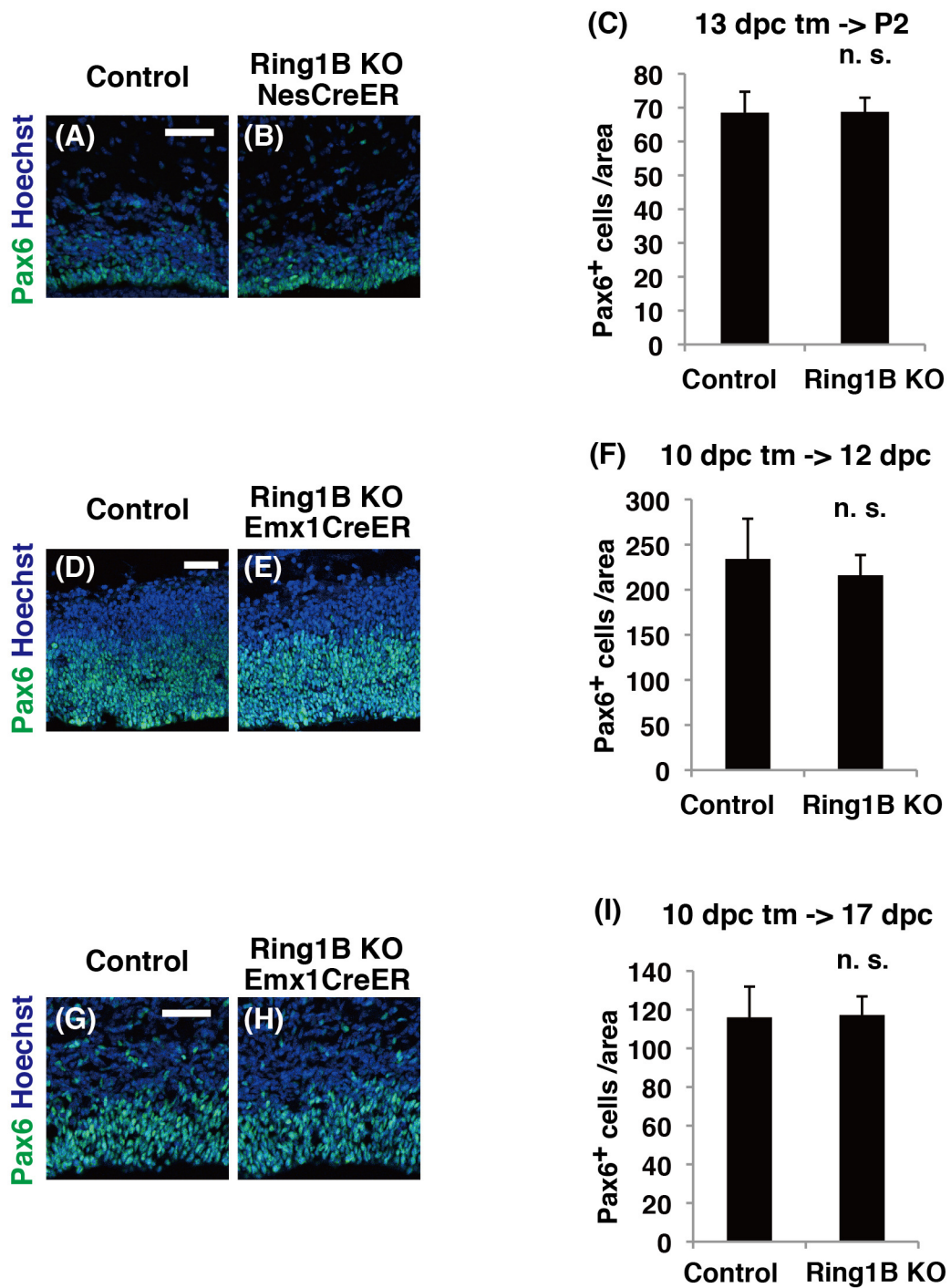
Supplemental Figure 2



Supplementary Figure 3

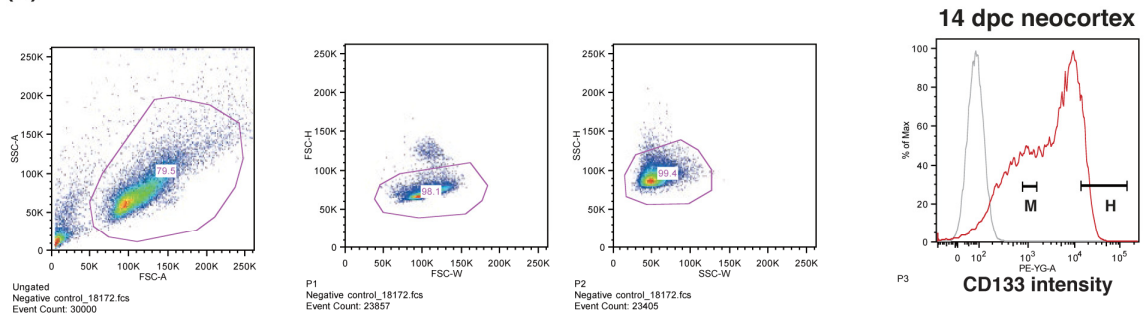


Supplemental Figure 4

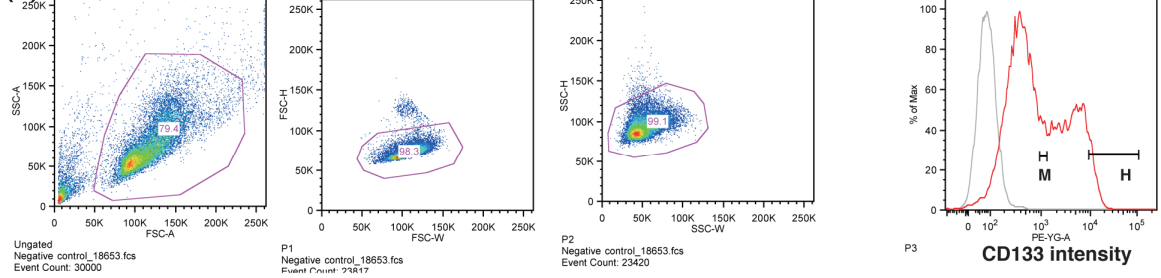


Supplemental Figure 5

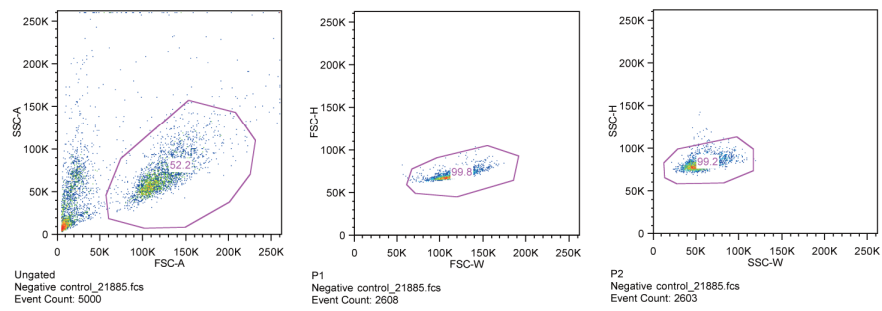
(A)



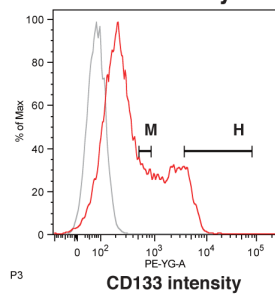
(B)



(C)

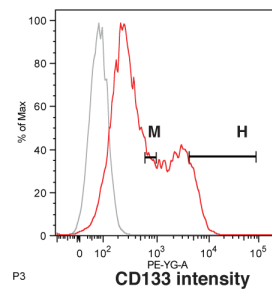


(D) Control embryo



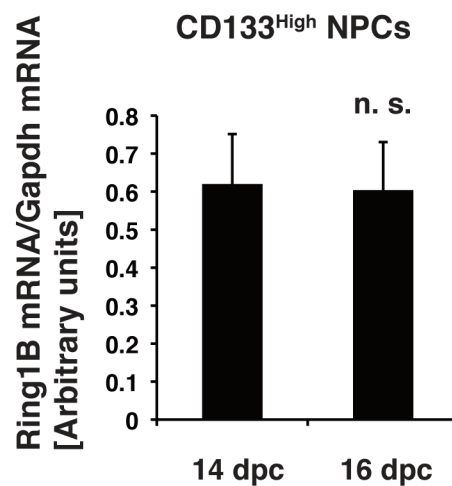
Sample	%
3_CD133_PE_21888.fcs	99.3
Negative control_21885.fcs	99.2

(E) Ring1B KO embryo

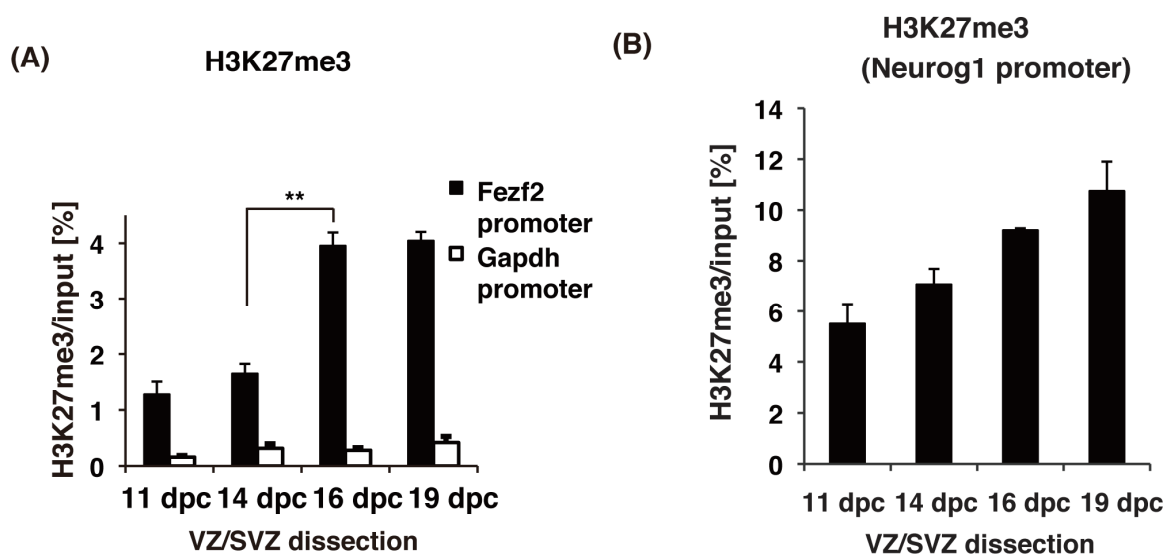


Sample	%
1_CD133_PE_21886.fcs	99.5
Negative control_21885.fcs	99.2

Supplemental Figure 6



Supplemental Figure 7



Supplementary Figure 8

